



Research paper

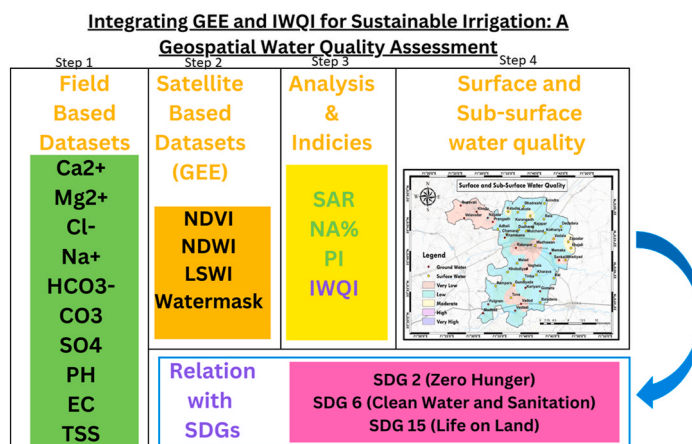
# Integrating GEE and IWQI for sustainable irrigation: A geospatial water quality assessment

Uttam Vyas<sup>a</sup>, Dhruvesh Patel<sup>a,\*</sup>, Vinay Vakharia<sup>b</sup>, Keval H. Jodhani<sup>a,c,\*\*</sup><sup>a</sup> Department of Civil Engineering, School of Technology, Pandit Deendayal Energy University, Gandhinagar, 382426, Gujarat, India<sup>b</sup> Department of Mechanical Engineering, School of Technology, Pandit Deendayal Energy University, Gandhinagar, 382426, Gujarat, India<sup>c</sup> Department of Civil Engineering, Institute of Technology, Nirma University, Ahmedabad, 382481, Gujarat, India

## HIGHLIGHTS

- Developed IWQI and GIS maps for groundwater irrigation suitability in Wadhwan, Gujarat.
- Mapped NDVI, NDWI, LSWI using Landsat; Watermask using Sentinel II via GEE.
- 29.54% of samples showed severe restrictions, suitable only for high salt tolerance plants.
- GIS zoning map identified “Red Zones” to guide sustainable groundwater management.

## GRAPHICAL ABSTRACT



## ARTICLE INFO

## Keywords:

Water quality

GEE

IWQI

Geospatial techniques

Sustainable water management

## ABSTRACT

The surface and sub-surface water quality is one of the decisive parameters for sustainable agriculture and water resources management. Deteriorating water quality impacts the irrigation, crop production, and human health. Therefore, the present work made an attempt to identify the water suitability for irrigation using the contemporary approach i.e. Irrigation Water Quality Index (IWQI) and Zone mapping using GIS techniques, and demonstrated for case of Wadhwan, Gujarat India. Three indices i.e., NDVI, NDWI, and LSWI were mapped using Landsat satellite imagery, whereas, Watermask index was mapped using Sentinel II satellite imagery for the assessment of the availability of water in different forms. The IWQI has applied to categorize the water quality as severe, high, moderate, low, and no restriction. The IWQI in the study area ranges from 6.4 to 62.5. The overall the water quality of study area shows that the 13.64 % of the region in severe restriction range, 56.82% in high restriction range, and 29.54% in moderate restriction range, which is in alarming for farmers and policy makers.

\* Corresponding author. Department of Civil Engineering, School of Technology, Pandit Deendayal Energy University, Gandhinagar, 382426, Gujarat, India.

\*\* Corresponding author. Department of Civil Engineering, Institute of Technology, Nirma University, Ahmedabad, 382481, Gujarat, India.

E-mail addresses: [Uttam.vphd21@sot.pdpu.ac.in](mailto:Uttam.vphd21@sot.pdpu.ac.in) (U. Vyas), [dhruvesh.patel@sot.pdpu.ac.in](mailto:dhruvesh.patel@sot.pdpu.ac.in) (D. Patel), [vinayvakharia4343@gmail.com](mailto:vinayvakharia4343@gmail.com) (V. Vakharia), [jodhanikeval@gmail.com](mailto:jodhanikeval@gmail.com) (K.H. Jodhani).<https://doi.org/10.1016/j.gsd.2024.101332>

Received 31 May 2024; Received in revised form 22 August 2024; Accepted 2 September 2024

Available online 5 September 2024

2352-801X/© 2024 Published by Elsevier B.V.

The GIS zoning map effectively visualized the spatial distribution of IWQI, helping decision-makers to identify severity zones. Furthermore, the Piper diagram analysis has been performed, which shows that the water quality of the study area falls under mixed  $\text{Ca}^{2+}\text{-Mg}^{2+}\text{-Cl}^-$ , mixed  $\text{Ca}^{2+}\text{-Na}^+\text{-HCO}_3^-$ , and  $\text{Na-HCO}_3^-$  types. The results revealed that major areas are in moderate to severe restriction zones, lying under deteriorated water quality, and need immediate attention for improvement before use. The IWQI advances SDG 2 (Zero Hunger) by optimizing water quality for crop production and SDG 6 (Clean Water and Sanitation) by ensuring sustainable water resource management, while indirectly supporting SDG 15 (Life on Land) through improved soil health and land management practices.

## 1. Introduction

Water quality remains a prominent issue globally, actuating governments to seek additional water resources to fulfil the needs of domestic, agricultural, and industrial sectors. The 2021 World Water Development Report, released by UNESCO, underscores a concerning trend: global freshwater consumption has surged six-fold over the last century, with a steady annual growth rate of about 1% since the 1980s. This escalating demand for water is exacerbating challenges to water quality. These challenging conditions jeopardize ecosystems and endanger human health and hinder sustainable social development efforts. Although water is readily accessible to a vast number of individuals worldwide, it is frequently deemed unsafe for consumption and insufficient to meet fundamental health requirements in diverse locations (Makubura et al., 2022). According to the World Health Organization, roughly 1.1 billion individuals worldwide consume unsafe water, with a significant portion of the world's diarrheal diseases being linked to unsafe water, inadequate sanitation, and unhygienic practices. Furthermore, the water supply sector confronts significant challenges stemming from climate change (Jodhani et al., 2024e; Gupta et al., 2021a), global warming, and urbanization (Gond et al., 2023a,b; N. Gupta et al., 2022). Inadequate quantity and subpar quality of water have profound ramifications for sustainable development, particularly in developing nations. Because pollution, whether physical or chemical, impacts the qualities of the water bodies it enters, increased human activity has a direct influence on water quality (Khaniya et al., 2021).

RS and GIS are essential tools in water quality assessment and management (Quinn et al., 2022). By integrating remote sensing data, with ground data from in situ water quality monitoring programs, researchers can establish quantitative frameworks to effectively monitor inland water quality (Tong et al., 2010). Remote sensing technologies, such as Landsat 8 images, are extensively used for water quality assessments, facilitating the mapping of parameters like turbidity and chlorophyll concentration in inland water bodies (Cruz-Montes et al., 2023). Research has demonstrated that the integration of remote sensing techniques with GIS can aid in evaluating water quality parameters and tracking changes in water quality over temporal and spatial scales (Gupta et al., 2021), offering valuable synoptic views of ambient water quality (Mohd Nazri et al., 2024). Remote sensing has proven effective in assessing water turbidity, soil moisture, water demand modeling, flood mapping, and groundwater management (Odermatt et al., 2018; Kaplan et al., 2019). The amalgamation of remote sensing and GIS has played a crucial role in groundwater assessments, assisting in the evaluation, monitoring, and conservation of groundwater resources (Rekha et al., 2011). Remote sensing technologies are widely employed to measure the available water bodies, including extreme conditions i.e., flood (Shivhare et al., 2016) and drought (Gupta et al., 2022; Gond et al., 2023a, 2023b) and chlorophyll-a levels also in inland water bodies (Hussein and Assaf 2020). By combining remote sensing, GIS, and traditional in situ sampling, a more comprehensive assessment of water quality parameters in various water systems can be achieved (Silva Filho et al., 2020).

Irrigation water quality is a crucial factor in agricultural productivity, and various indices are used to evaluate its suitability for irrigation (Usali and Ismail 2010). The SAR is a key parameter in assessing

irrigation water quality. High levels of sodium in irrigation water can lead to soil degradation over time (Solomon et al., 2020). Additionally, the PI is another significant indicator used to determine water suitability for irrigation (Shil et al., 2019). Moreover, the IWQI is a comprehensive tool that combines different water quality parameters to provide a single numerical expression for assessing water suitability for irrigation (El-Amier et al., 2021). To estimate overall irrigation water quality, IWQI takes into account SAR, sodium percentage, residual sodium carbonate, magnesium ratio, Kelly index, potential salinity, and other indicators (El-Amier et al., 2021). In addition to SAR, groundwater quality for irrigation is assessed using indices such as soluble sodium percentage, magnesium adsorption ratio, residual sodium carbonate, and Kelly's ratio. These indices provide a full knowledge of water appropriateness for irrigation, taking into account aspects that might affect soil structure and plant development. In many research, irrigation water quality is evaluated using different indices such as SAR, PI, and IWQI to determine water compatibility with agricultural techniques (Omar et al., 2020). These indicators are critical for understanding the possible influence of water quality on soil health, crop output, and agricultural sustainability.

Water quality assessment is a crucial component of environmental monitoring, and the utilization of satellite-derived indices is pivotal in this field. Several studies have investigated the effectiveness of various indices such as NDVI, NDWI, WRI, and LSWI for water quality assessment (Rokni et al., 2014; Acharya et al. 2018, 2019). These indices have been employed to extract surface water from the GEE platform, and satellite data, monitor changes in vegetation dynamics, and assess the extent of water bodies over time (Dervisoglu 2021; Albarqouni et al., 2022; Jodhani et al., 2024c). The use of satellite imagery, particularly from platforms like GEE, has facilitated the effective monitoring of water quality parameters. Research has demonstrated a high correlation between the visible and near-infrared spectral bands with in-situ measurements, making them valuable for water quality monitoring (Khan et al., 2021). Additionally, GEE has been instrumental in evaluating drought indices, temperature variations, soil moisture conditions, and precipitation patterns using satellite-derived data (Omar et al., 2022). Numerous studies have focused on assessing surface water dynamics and changes in water bodies through satellite imagery and remote sensing techniques (Zhang et al., 2018; Liuzzo et al., 2020). These indices have proven effective in delineating surface water bodies, monitoring floods (Jodhani et al., 2023b), erosion (Jodhani et al., 2023c), air quality (Jodhani et al., 2024c), fire (Jodhani et al., 2024a), and detecting fluctuations in water levels. Moreover, the integration of multiple indices like NDVI, NDWI, MNDWI, and WRI has been demonstrated to enhance the sensitivity of water body detection (Jodhani et al., 2024d), particularly in mixed water and vegetation pixels (Acharya et al., 2018). This integrated approach offers a comprehensive method for surface water extraction and monitoring using Landsat imagery (Acharya et al., 2019). The adoption of satellite-derived indices such as NDVI, NDWI, and LSWI, in conjunction with platforms like GEE (Jodhani et al. 2023a, 2024b), has significantly advanced water quality assessment and monitoring (Gujrati and Jha 2018; Sha et al., 2022). These indices provide valuable insights into surface water dynamics, changes in vegetation, and environmental quality, thereby contributing to improved water resource management (Jodhani et al., 2021).

The number of researchers has attempted and utilised the various indexes and satellite data for water quality assessment and irrigation suitability, however, none of them have comprehensively used the IWQI, GEE derived NDVI, NDWI, LSWI and watermask for water quality assessment, irrigation suitability and linked it with SDGs. Therefore, present research aim to utilize the contemporary comprehensive techniques for water quality assessment and irrigation suitability, and linked it with SDGs, which was not attended ever before in any literature. This novel approach addresses knowledge gaps by integrating a comprehensive methodology for utilizing Google Earth Engine derived indices in relation to the Irrigation Water Quality Index and its alignment with the Sustainable Development Goals. To demonstrate the approach further, Wadhwan, Gujarat India has been taken as case study. The study attend the classification of water suitability using both ground and satellite data for better sustainable water management practices. The main objectives of the study are 1) Assessing physio-chemical parameters based on ground datasets. 2) Mapping and analysing various indices (NDVI, NDWI, LSWI) using Landsat 8 satellite datasets and water masks using Sentinel-II datasets. 3) Determining assessment parameters: IWQI, SAR, and PI. 4) Classifying water quality and its suitability for irrigation. These comprehensive techniques/integrated approach provide detailed spatial and temporal insights into water availability and soil health, guiding targeted policy decisions and sustainable practices. Policy-makers should use these integrated insights to address local challenges, while researchers should further refine and validate these methods to enhance water management strategies. Furthermore, the recommendations provided are closely aligned with the United Nations Sustainable Development Goals (SDGs). The Irrigation Water Quality Index directly contributes to SDG 2 (Zero Hunger) by optimizing water quality for enhanced agricultural productivity. It also supports SDG 6 (Clean Water and Sanitation) by promoting sustainable water resource management. Additionally, by fostering better soil health and land management practices, the index indirectly aids in achieving SDG 15 (Life on Land). It supports sustainable agriculture, promotes health and well-being, conserves water resources, and protects ecosystems both on land and in water.

## 2. Study area

Location map of Wadhwan region, Gujarat, India is illustrated in Fig. 1. It is an agriculturally rich region located on the banks of the Bhogavo River at approximately 22°30" to 22°50" N latitude and 71°25" to 71°50" E longitude, and an average annual rainfall of about 500 mm, predominantly occurring during the monsoon season from June to September (Fig. 1). The region experiences a semi-arid climate, characterized by scorching summers, mild winters, and scanty rainfall. The summer months, extending from March to June, are typically hot and dry, with temperatures soaring above 40 °C. Monsoon rains bring relief from the sweltering heat from July to September, although precipitation levels are relatively low compared to other regions of India. Winter, spanning from November to February, is mild and pleasant, with temperatures averaging around 15–25 °C. Despite its arid climate, Wadhwan's unique location and topography contribute to its ecological diversity and significance. The topography of Wadhwan is primarily flat with some undulating terrain, and the soil varies from sandy loam to clayey, influencing the types of crops cultivated and irrigation practices used. Cotton, wheat, bajra (pearl millet), pulses, and vegetables are the most common crops farmed in Wadhwan. Agriculture in this area relies significantly on irrigation, with groundwater serving as the major supply, supported by the Bhogavo River. Providing high-quality irrigation water encourages sustainable farming practices, increases crop yields, and improves the health and well-being of the local community by lowering the dangers connected with polluted water sources. Furthermore, good water management measures may assist reduce water shortages and safeguard critical water resources, so adding to the agricultural system's overall sustainability and resilience. By addressing the unique difficulties and possibilities in Wadhwan, research and development initiatives may create effective solutions to enhance water management, promote sustainable agricultural growth, and contribute to the larger objectives of regional and national sustainability. This comprehensive strategy coincides with the SDGs since it promotes food security, economic development, and environmental preservation in Wadhwan.

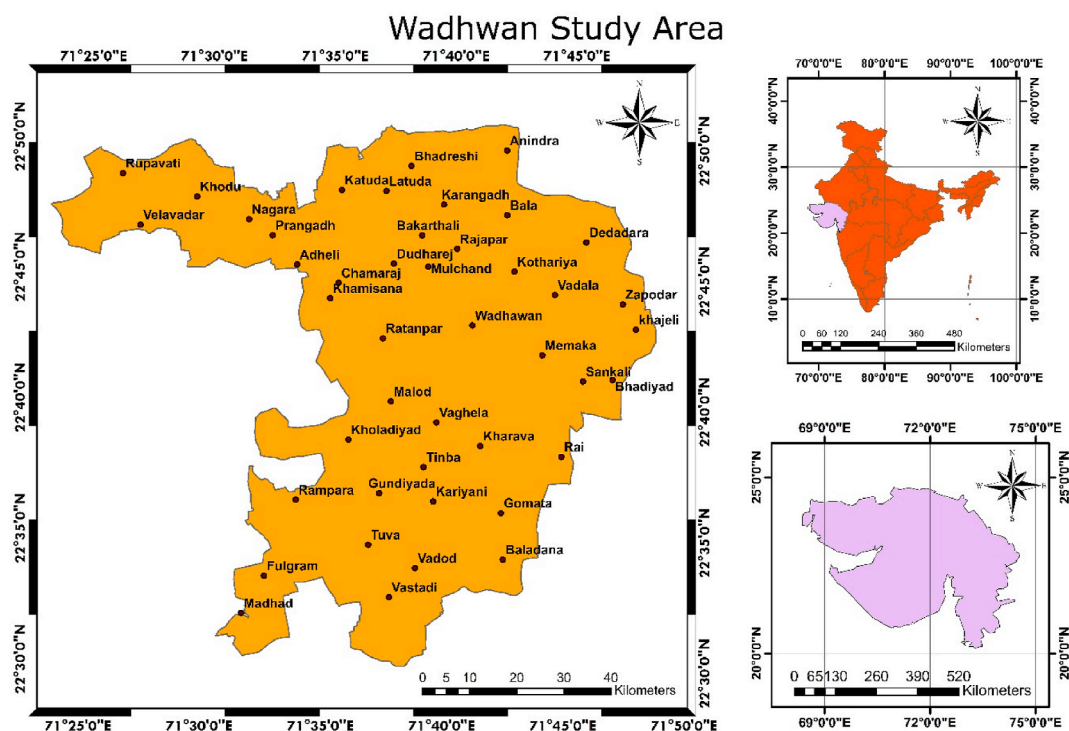


Fig. 1. Wadhwan region as Study area, and its location with respect to Gujarat and India.

### 3. Materials and methods

The materials and techniques used in this research enabled a full evaluation of water quality in Wadhwan, Gujarat. Field data collecting, laboratory analysis, GIS mapping, and statistical analysis approaches were used to acquire important insights into the research area’s hydrogeological features and difficulties. The results improve our knowledge of water quality dynamics, allowing us to make more informed decisions about sustainable water resource management and environmental protection in Wadhwan and other comparable places. Wadhwan’s hydrogeological framework consists of both alluvial aquifers along river valleys and fractured rock aquifers inside sedimentary strata. Groundwater is the principal source of water supply for household, agricultural, and industrial applications. The Bhogavo River and its tributaries act as important groundwater recharge areas, refilling aquifers during the monsoon season. Natural and anthropogenic pollutants such as fluoride, nitrate, and salt affect groundwater quality, causing threats to human health and water security. Fig. 2 depicts a flow chart for assessing the quality of ground and surface water used for irrigation.

The procedures used for water quality evaluation are described, as field surveys were carried out to collect water samples from different places within the research region. Hydrogeological factors, land use patterns, and probable pollution sources all played a role in selecting sampling locations. Water samples were tested for critical metrics such as magnesium content, salt percentage, sulphate concentration, SAR, and PI. Na% and IWQI were determined using the obtained values. GEE was hired to get Landsat 8 and Sentinel 2 datasets for optioning NDVI,

NDWI, LSWI, and Watermask index. The spatial distribution maps of water quality metrics were created using GIS software. GIS mapping enabled the visualization and analysis of spatial patterns, assisting in the identification of possible hotspots and regions of concern.

#### 3.1. Sodium adsorption ratio (SAR)

The SAR value of irrigation water is used to quantify the relative proportions of sodium ( $Na^+$ ) to calcium ( $Ca^{2+}$ ), and magnesium ( $Mg^{2+}$ ) respectively (Singh et al., 2021). Moreover, it was determined through equation (1) by applying the below equation (1):

$$SAR = \sqrt{2} \frac{Na^+}{\sqrt{Ca^{2+} + Mg^{2+}}} \quad (1)$$

Where,

$Na^+$ ,  $Ca^{2+}$ , and  $Mg^{2+}$  are the concentrations of sodium, calcium, and magnesium ions present in the water.

The unit of SAR is in milli equivalents per litre (mEq/L)<sup>1/2</sup>. Table 1 illustrates the values of SAR for the Wadhwan region.

#### 3.2. Sodium percent (%Na)

The sodium percent is a significant parameter that is well known for its application in irrigation purposes, and it is used for the evaluation of groundwater quality. A renowned classification developed by (Wilcox 1955) was documented and used in the literature for a prolonged period of time. The classification of groundwater quality is centred around five

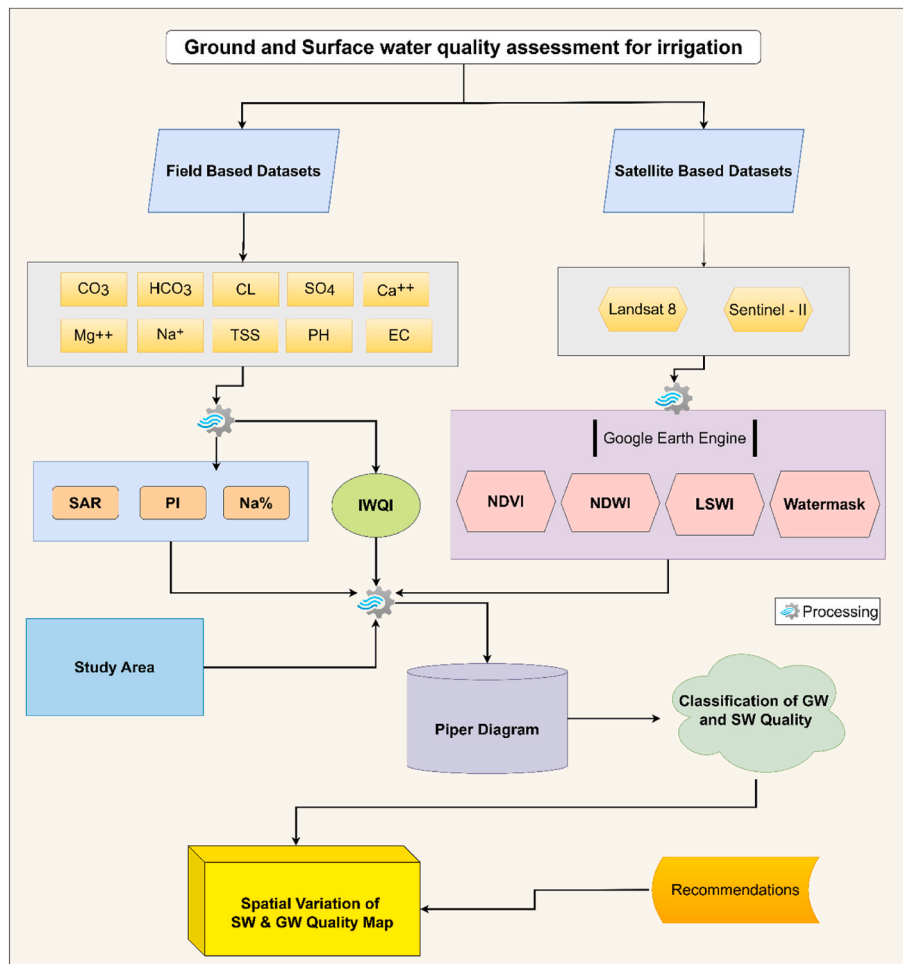


Fig. 2. Flow Chart for ground and surface water quality assessment for irrigation.

**Table 1**

Represents the proposed limiting values for irrigation water quality parameters (Spandana et al., 2013; Abbasnia et al., 2018).

Si	HCO <sub>3</sub> (meq/L)	Cl (meq/ L)	SAR (meq/ L) <sup>1/2</sup>	Na (meq/ L)	EC (µmho/ cm)
85–100	1–1.5	<4	<3	2–3	200–750
60–85	1.5–4.5	4–7	3–6	3–6	750–1500
35–60	4.5–8.5	7–10	6–12	6–12	1500–3000
0–35	<1 or >8.5	>10	>12	>12	<200 or >3000

classes (Maliqi et al., 2020; Yıldız and Karakuş 2020): excellent water having a range of 0 ≤ %Na ≤20%, good water ranging between 20% < %Na ≤40%, permissible between 40% < %Na ≤60%, doubtful having 60% < %Na ≤80%, and unsuitable lying between 80% < %Na ≤100 respectively. On the basis of this classification, the %Na was calculated through equation (2):

$$Na\% = \frac{(Na^+)}{(Ca^{+2} + Mg^{+2} + Na^+)} * 100 \tag{2}$$

Where,

Na<sup>+</sup>, Ca<sup>2+</sup>, and Mg<sup>2+</sup> are the concentrations of sodium, calcium, and magnesium cations present in the water in mEq/L. (The results are provided in Table 1)

### 3.3. Permeability index (PI)

The permeability index (PI) developed by (Doneen 1964), is also a well-known parameter for the suitability of irrigation water. Long-term usage of irrigation water influences PI (with high levels of concentration for salts) as it is affected by the Na<sup>+</sup>, Ca<sup>2+</sup>, Mg<sup>2+</sup>, and HCO<sub>3</sub><sup>-</sup> ions of the soil (Rawat et al., 2018a). PI was calculated as shown in equation (3):

$$PI = \frac{Na^+ + \sqrt{HCO_3^-}}{Ca^{2+} + Mg^{2+} + Na^+} * 100 \tag{3}$$

where,

Na<sup>+</sup>, Ca<sup>2+</sup>, Mg<sup>2+</sup> and HCO<sub>3</sub><sup>-</sup> are the concentrations of sodium, calcium magnesium cations, and bicarbonate ions present in the water in mEq/L.

### 3.4. Irrigation Water Quality Index (IWQI)

The IWQI is calculated through the following equation (5) for water quality parameters namely, SAR, HCO<sub>3</sub><sup>-</sup>, Cl<sup>-</sup>, Na<sup>+</sup> and EC (Abbasnia et al., 2018; Rawat et al., 2018b). The measurement values for water quality parameters S<sub>i</sub> was calculated and the weightage values were considered as per the table. Further, the table provides the details regarding irrigation water quality parameters and the proposed limiting values assigned to them respectively (Spandana et al., 2013; Abbasnia et al., 2018).

The values for S<sub>i</sub> (quality of each parameter) were calculated through the below equation (4) for each of the five water quality parameters namely sEC, sSAR, sNa, sCl, sHCO<sub>3</sub> and the sample data values are represented in the table. In this formula the s<sub>iam</sub> is considered the highest limiting value of the parameter’s range as shown in Table 1.

$$S_i = S_{max} - \left( \frac{(z_{ij} - z_{iv}) \times S_{iam}}{z_{am}} \right) \tag{4}$$

Where,

S<sub>max</sub> is the upper value of the corresponding S<sub>i</sub> class  
 z<sub>ij</sub> demonstrates the field data collection values (observed value) as shown in Table 3  
 z<sub>iv</sub> represents the lower limit value of the observed parameters’ class  
 S<sub>iam</sub> corresponds to the class amplitude of the S<sub>i</sub> class

z<sub>am</sub> refers to the class amplitude to which the parameter belongs.

Lastly, the IWQI was calculated using the below equation (5). Here, the values of S<sub>i</sub> were multiplied using the assigned weights of each parameter as listed in Table 2 (Meireles et al., 2010)

$$IWQI = \sum_1^p S_i W_i \tag{5}$$

Where,

p refers to the number of parameters considered (here, five are considered)

S<sub>i</sub> represents the quality of each parameter

W<sub>i</sub> is the weightage values allocated to each parameters.

## 4. Results and discussion

This research assessed groundwater quality using the IWQI, SAR, % Na, EC, and Cl-. The data for each characteristic was visually represented using GIS zoning maps. GIS-based IWQI maps help local governments and stakeholders make better decisions by displaying spatial changes in water quality across areas (Acharya et al., 2024). These maps allow for optimum resource allocation by identifying appropriate irrigation regions and prioritizing interventions such as water quality improvement projects and infrastructure improvements. Stakeholders may utilize IWQI maps to make intelligent decisions about agricultural practices, land use planning, and environmental management, maximizing water resources while taking into account quality limits. Real-time monitoring enabled by GIS aids in tracking IWQI trends, evaluating the effect of adopted interventions, and ensuring compliance with water quality requirements (Acharya et al., 2024). Additionally, these maps aid in emergency response efforts by quickly identifying areas affected by water quality issues, enhancing resilience, and promoting sustainable water management practices among communities. The findings from the investigation of magnesium concentration, salt percentage, sulphate concentration, SAR, and PI indicate detailed spatial patterns and environmental dynamics in the studied region. Elevated magnesium and sulphate concentrations in certain areas point to probable human impacts on soil and water quality, such as industrial discharge or agricultural runoff. The geographical distribution of salt percentage identifies areas prone to salinity problems, especially in areas impacted by irrigation techniques and soil type. Similarly, SAR values indicate varying degrees of soil salinity across the landscape, emphasizing the importance of sustainable irrigation management to mitigate adverse impacts on crop productivity and soil health (Rawat and Singh 2018; Maliqi et al., 2023). Additionally, the analysis of PI values underscores the significance of soil permeability in regulating water infiltration and runoff, with implications for flood risk management and soil conservation practices (Kumar Pradhan et al., 2020; Kumar and Singh 2021). Ensuring that irrigation water meets high standards not only supports food security and public health but also contributes to the resilience and sustainability of our natural environment, reinforcing the interconnected nature of the SDGs and the pivotal role that water quality plays in achieving them.

**Table 2**

Illustrates the weightage values for each of the IWQI parameters (Meireles et al., 2010).

Abbreviation	Parameters	Weights (W <sub>i</sub> )
HCO <sub>3</sub> <sup>-</sup>	Bicarbonate ion	0.202
Cl <sup>-</sup>	Chloride ion	0.194
SAR	Sodium Adsorption Ratio	0.189
Na <sup>+</sup>	Sodium ion	0.204
EC	Electrical conductivity	0.211
	<b>Total</b>	<b>1.000</b>

4.1. Land surface water index (LSWI)

The LSWI employing GEE exhibited considerable geographical and temporal changes in water presence throughout the research region. By analyzing Landsat 8 images from January to December 2020, researchers created a time series of LSWI values that highlighted times of elevated water content in the area. The index was assessed using both qualitative visual inspection and quantitative accuracy measures of total correctness. The GIS zoning maps showed that areas with high LSWI values, indicating high moisture content, were mostly situated near water bodies and irrigated fields, while lower LSWI values linked to dry zones and non-irrigated regions. The time series graphic revealed different seasonal tendencies, with greater LSWI values during monsoon months and lower values during summer months, indicating regional climate patterns. A number larger than 0.1 often indicates that the vegetation is healthy and well-watered, or that there is surface water available. The northern area with the lower LSWI denotes a drier environment, whereas the southern region with the higher LSWI indicates a wetter zone (Fig. 3a). This investigation gives vital insights into the study area's hydrological dynamics, which will help with water resource management and agricultural planning.

4.2. Normalized difference vegetation index (NDVI)

The findings of computing the NDVI using GEE provided vital information on vegetation health and distribution across the research area. A comprehensive time series of NDVI values was produced by utilizing Landsat 8 imagery from January 2020 to December 2020, which emphasized the temporal variations in vegetation greenness. The NDVI maps indicated that areas with high NDVI values, representing healthy and dense vegetation, were concentrated in forested regions and agricultural zones, whereas lower NDVI values were found in urban areas, barren lands, and water bodies (Feng et al., 2023). The time series chart displayed clear seasonal trends, with NDVI peaking during the growing seasons and declining during the dormant or dry periods (Makubura et al., 2022). Most of the part lies in the range of 0.25–0.75 and these values indicate sparse vegetation such as shrubs, grasslands, or croplands. The vegetation is typically less dense and may be under stress. However, central region has a range of 0.1–0.25 and these values generally correspond to barren areas of rock, sand, or snow. There is very little to no vegetation Fig. 3 b. This detailed analysis of NDVI provides crucial information for monitoring vegetation dynamics, supporting agricultural management, and informing sustainable land-use planning.

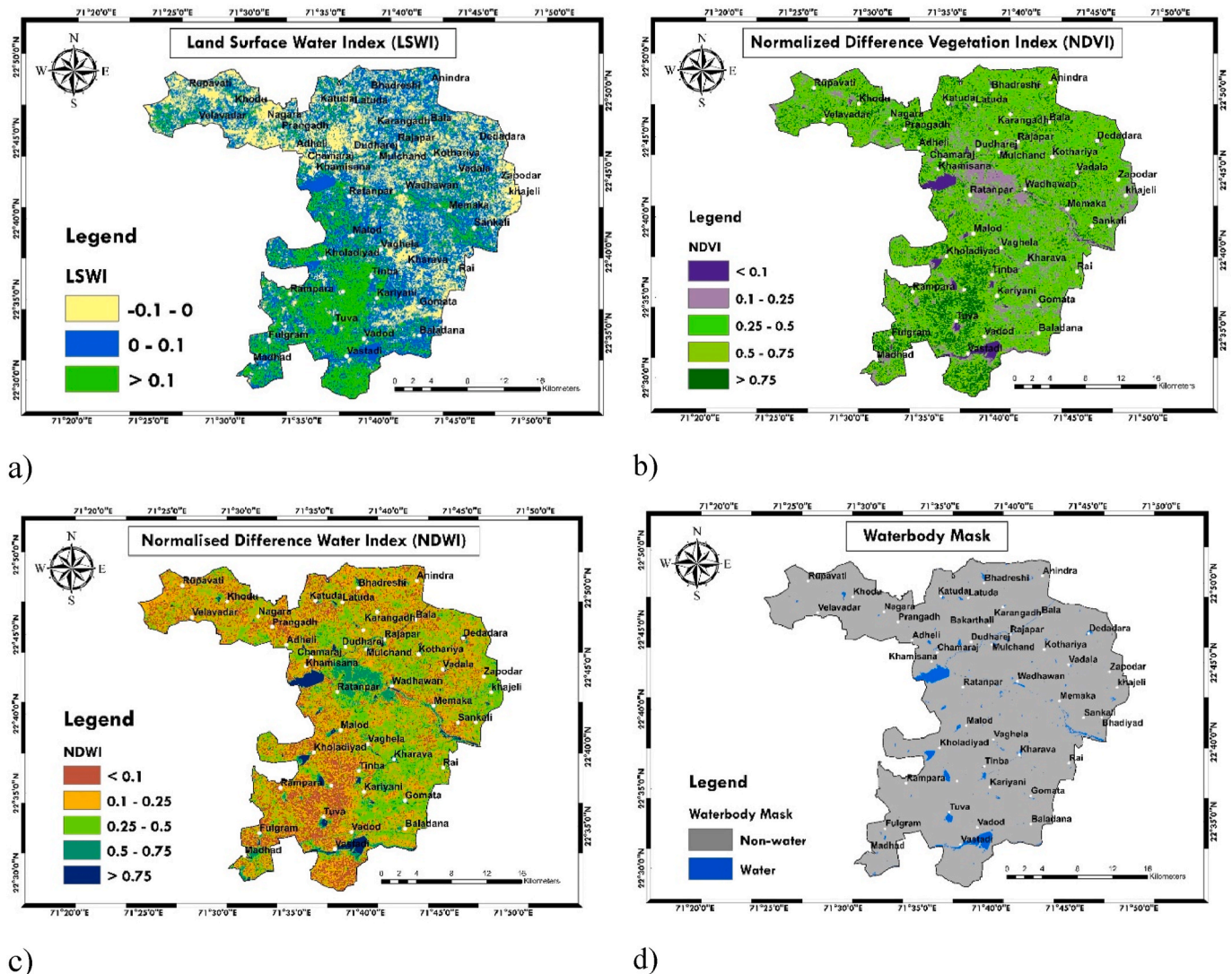


Fig. 3. Spatial variation in GEE derived indices a) LSWI b) NDVI c) NDWI d) Waterbody mask.

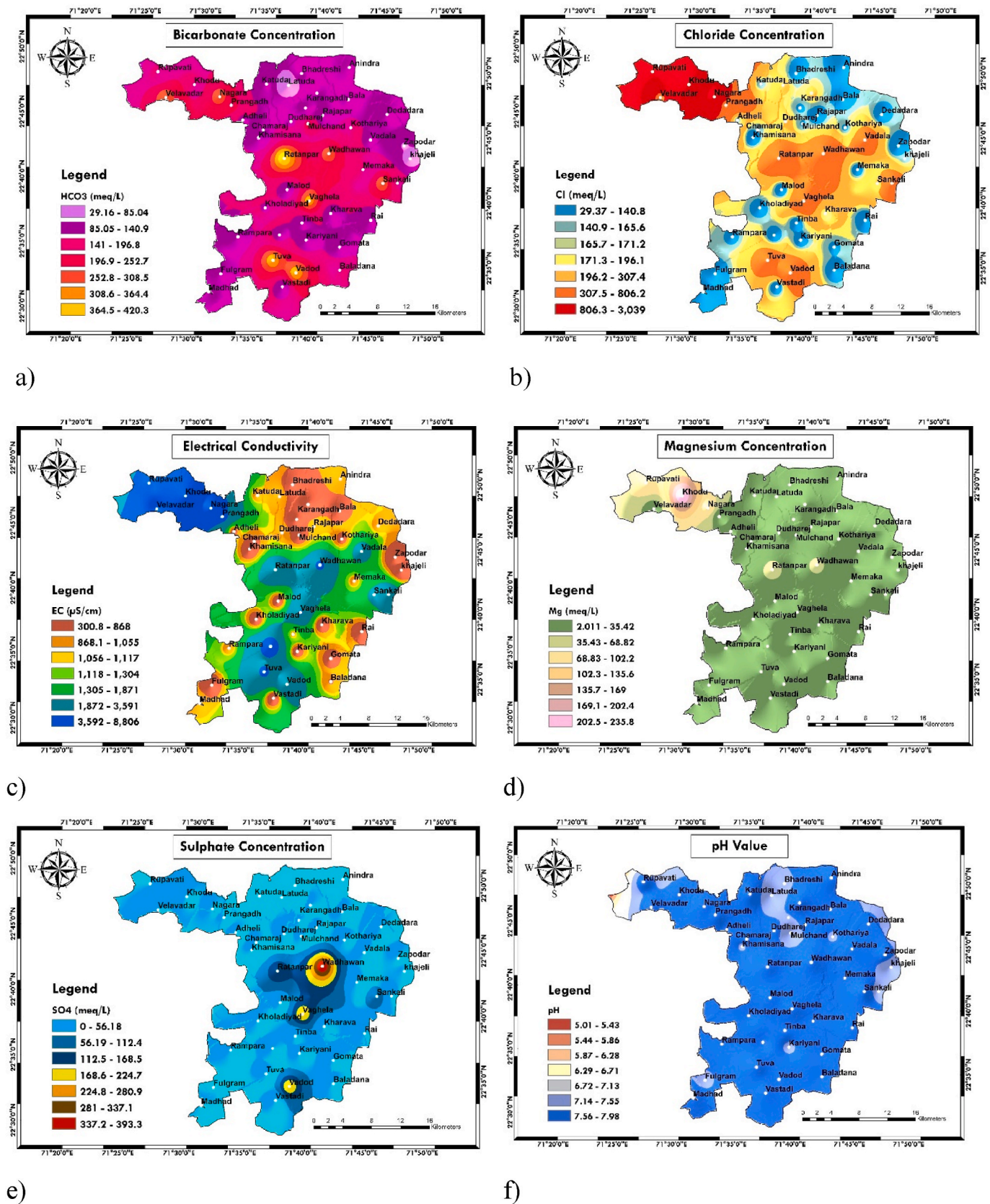
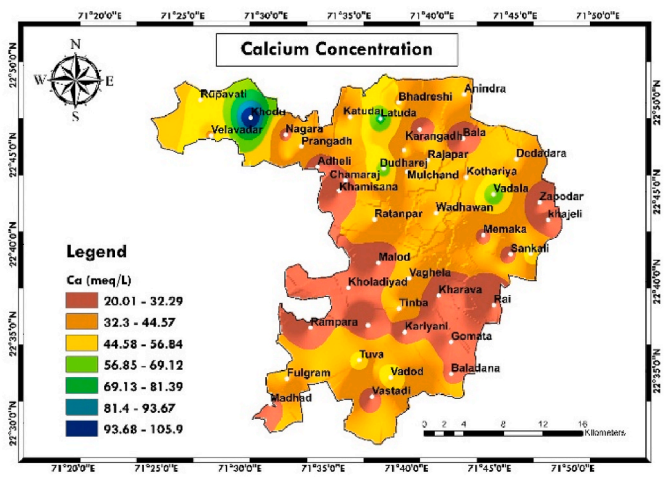
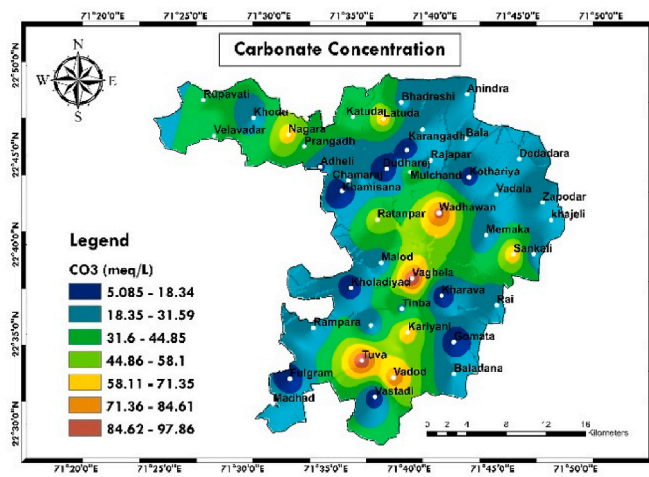
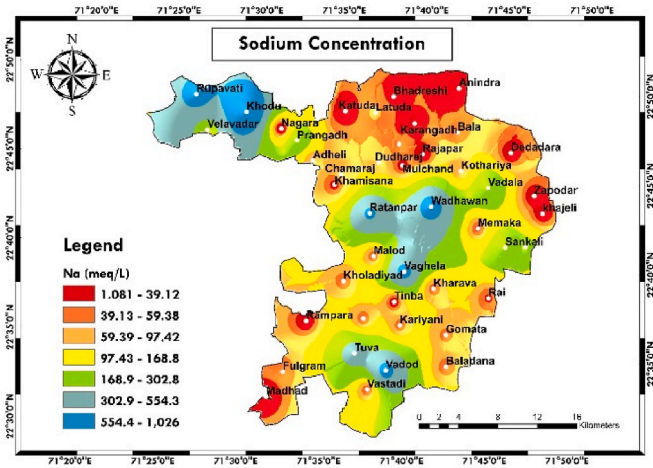
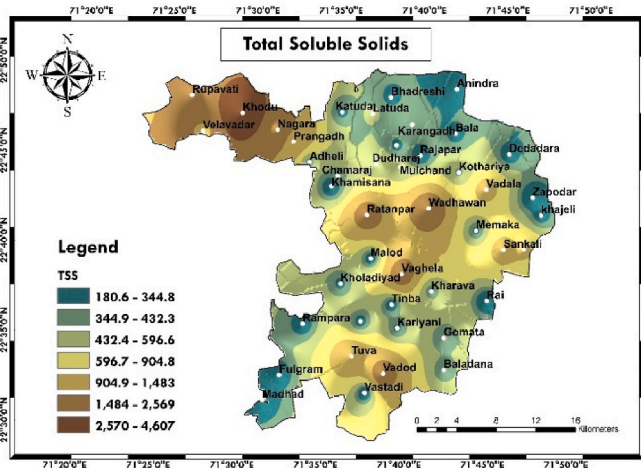


Fig. 4. Spatial variation in a) bicarbonate concentration b) Chloride concentration, c) Electrical conductivity, d) Magnesium concentration, e) sulphate concentration f) pH value g) Carbonate concentration h) Calcium concentration i) Total soluble solids j) Sodium concentration.



g)

h)



i)

j)

Fig. 4. (continued).

### 4.3. Normalized difference water index (NDWI)

The results of calculating the NDWI using GEE provided valuable insights into water content and distribution across the study area. By analyzing Landsat 8 imagery from January 2020 to December 2020, a time series of NDWI values generated, capturing the spatial and temporal variations in surface water. The NDWI maps showed that areas with high NDWI values, indicating high water content, were primarily located near rivers, lakes, and wetlands, while lower NDWI values were associated with dry regions, urban areas, and vegetation. The time series chart revealed distinct seasonal trends, with higher NDWI values corresponding to wetter periods and lower values during drier seasons (Khaniya et al., 2021). The values less than 0.1 values generally indicate non-water surfaces such as bare soil, built-up areas, or dry vegetation. The range between 0.1 and 0.25 represents areas with low water content, such as dry or sparse vegetation. The range 0.25–0.5 indicates moderate water content, typically associated with moist soil or vegetation that is well-watered but not saturated, and more than 0.5 signifies high water content, such as open water bodies (lakes, rivers, reservoirs), wetlands, or very well-irrigated vegetation Fig. 3 c. This analysis offers critical information for water resource management, flood monitoring, and environmental planning, aiding in the sustainable management of

water resources in the region.

### 4.4. Waterbody mask

In the findings section, the waterbody mask created using Sentinel-2 satellite data indicated the geographical distribution of surface water bodies in the research region. Using the NDWI derived from Sentinel-2 data, water pixels were separated from land pixels using a specified threshold. The resultant waterbody mask gave a thorough view of lakes, rivers, and other aquatic features across the terrain. The mask is useful for hydrological modeling, habitat evaluation, and water resource management since it properly delineates water bodies. The waterbody mask also helps to identify possible flood-prone locations and assists environmental monitoring activities (Karmakar et al., 2023). This study emphasizes the use of Sentinel-2 data for mapping and monitoring surface water dynamics at the regional scale. The blue color indicates the water body, whereas the gray color depicts the non-water body (Fig. 3d).



#### 4.5. Field data collection

##### 4.5.1. Bicarbonate concentration

The spatial distribution of bicarbonate concentration, based on field-collected data, revealed significant variability across the study area. High concentrations of bicarbonate were predominantly found in regions with intensive agricultural activities, likely due to the use of irrigation water with high bicarbonate levels and the natural geochemical processes in these areas. Conversely, lower bicarbonate concentrations were observed in less cultivated or urban regions, indicating different sources and dynamics of bicarbonate in groundwater. The GIS-based maps gave a clear visual representation of these trends, emphasizing zones with potentially problematic bicarbonate levels that might affect soil quality and crop health. Bicarbonates offer water a nice odor and have no influence on agriculture. The middle and southern regions of the research area have a high concentration of bicarbonates, while the northern half has a lower concentration (Fig. 4a). This precise geographical analysis is critical for designing targeted water management strategies and guaranteeing sustainable agricultural practices by focusing on regions with high bicarbonate concentrations.

##### 4.5.2. Chloride concentration

The geographical distribution of chloride concentration, as determined from data gathered in the field, showed significant diversity across the study region. Elevated chloride levels were primarily observed in coastal regions and areas with intensive agricultural activity, suggesting influences from seawater intrusion and the use of chloride-rich fertilizers or irrigation water. In contrast, lower chloride concentrations were found in inland and less cultivated areas, reflecting different hydrogeological conditions and minimal anthropogenic impact. The GIS-based maps effectively visualized these patterns, identifying critical zones where high chloride concentrations could pose risks to soil health and agricultural productivity. The north-western region has a high level of chloride concentration whereas, the remaining parts illustrate the average to lower concentration of chloride (Fig. 4 b). A major portion of the study area is in higher range of chloride concentration compared to its acceptable range (Nemčić-Jurec et al., 2019; Hussein et al., 2024) This comprehensive spatial analysis is essential for guiding water resource management and developing strategies to mitigate the impact of high chloride levels on the environment and agriculture.

##### 4.5.3. Electrical conductivity

The study area exhibited substantial variations in the spatial distribution of electrical conductivity (EC), as determined by field-collected data. Elevated EC levels were predominantly observed in regions characterized by intensive agricultural practices, urbanization, and industrial activities, indicating potential contamination from fertilizers, wastewater, and industrial effluents. Conversely, lower EC values were evident in less developed or natural areas, reflecting minimal anthropogenic influence and the presence of pristine water sources. The GIS-based mapping facilitated a clear visualization of these EC patterns, enabling the identification of hotspots where water quality might be compromised. This spatial analysis serves as a crucial tool for implementing targeted measures to mitigate EC-related risks and safeguard water resources for agricultural, ecological, and human uses. The limiting values of electrical conductivity were proposed for IWQI for classification (Rawat et al., 2019; Batarseh et al., 2021). The north-western region of the study area represents a very high electrical conductivity (3592–8806  $\mu\text{S}/\text{cm}$ ) whereas the remaining part illustrates the low to average electrical conductivity (Fig. 4 c).

##### 4.5.4. Magnesium concentration

An investigation of the regional distribution of magnesium content, using data acquired in the field, showed interesting patterns across the research area. Specific places, especially those with certain geological

formations or close to human activity like mining or industrial operations, have a significant abundance of magnesium in high quantities. Conversely, areas with lower magnesium concentrations were typically observed in more pristine environments or regions with limited human disturbance. The spatial maps generated from field data effectively visualized these variations, offering insights into the geological and anthropogenic factors influencing magnesium distribution. This detailed spatial analysis provides valuable information for understanding groundwater quality dynamics and identifying potential areas of concern for water resource management and environmental protection efforts. Additionally, it underscores the importance of targeted monitoring and mitigation strategies to address elevated magnesium levels in specific locations, ensuring the sustainability of water resources for both human and ecological needs. Magnesium is crucially important for plant growth, as it is a nutrient with several important functions, including its roles as a constituent of chlorophyll and an activation agent of enzymes (Qadir et al., 2018). The north-western region of the study area represents a very high magnesium concentration whereas the remaining part illustrates the magnesium concentration (Fig. 4 d).

##### 4.5.5. Sulphate concentration

The analysis of geographical patterns in sulphate concentration, generated from field data, revealed intriguing tendencies across the research region. The sulphate concentrations are within the FAO recommended range of 20 meq/L (Hussein et al., 2024). Sulphate concentrations rose noticeably in some areas, which were often linked to human activities like industrial discharge or agricultural runoff. These areas exhibited higher levels of sulphate in the soil and water, likely stemming from industrial processes, mining activities, or the application of sulphur-containing fertilizers. Conversely, lower sulphate concentrations were typically found in less impacted or natural environments. The spatial maps generated from field data effectively illustrated these variations, providing valuable insights into the spatial distribution of sulphate contamination. This detailed spatial analysis offers critical information for environmental monitoring and management efforts, highlighting areas of concern and guiding targeted mitigation strategies to protect water quality and ecosystem health. The central part of the study area represents a very high sulphate concentration whereas the remaining part illustrates a low to medium sulphate concentration (Fig. 4 e).

##### 4.5.6. pH value

The geographic distribution of pH values in field-collected water data exhibits significant acidity and alkalinity differences across sample locations. Geological formations, land use patterns, pollution sources, and natural water body characteristics all play a role in this variety. In some areas, lower pH values indicate acidic conditions, possibly due to industrial runoff, acid rain, or decomposing organic matter, which can adversely affect aquatic life and water usability. Other regions with higher pH values suggest alkaline conditions, potentially caused by the leaching of alkaline soils or the presence of certain minerals. Mapping these pH variations provides a visual representation of the water quality across the field, highlighting areas that may require intervention, such as neutralization treatments or pollution source mitigation. Understanding this spatial distribution is crucial for resource management, as it allows for targeted approaches to improve and maintain water quality, ensuring it meets the required standards for its intended use. Apart from the northwest corner region of the study area, the pH values were in the acceptable range (Fig. 4 f).

##### 4.5.7. Carbonate ( $\text{CO}_3$ )

Using field-collected water samples to look at how carbonate concentration changes over space shows different trends of alkalinity at different sampling sites. Higher carbonate concentrations in some places mean that there are more dissolved carbonates and bicarbonates. This could be because of natural factors, like the presence of limestone or

dolomite, or because of human activities, like applying lime to farms. The water in these places tends to have more alkaline pH levels, which makes it better at protecting against acidity. In contrast, regions with lower carbonate concentrations may reflect acidic conditions or a lack of carbonate-bearing minerals in the underlying geology. Such areas might be more vulnerable to pH fluctuations due to acid rain, organic matter decomposition, or industrial runoff, leading to lower pH values.

Mapping the spatial distribution of carbonate concentrations provides valuable insights into the water chemistry and its underlying causes. This information is crucial for targeted water management strategies, including the need for lime additions in agriculture, monitoring potential pollution sources, and protecting aquatic ecosystems. The carbonate concentration varies in the range of 5–98. The higher concentration is represented in the red color majorly in Wadhawan, Vaghela, Tuva, Nagara, Kariyani, and Sankeli whereas, the lower concentration is represented in green to blue color covers the remaining region of the study area (92%) (Fig. 4 g).

#### 4.5.8. Calcium concentration

There are notable variations in mineral content across different places, impacted by both natural geology and human activity, as shown by the geographic fluctuation in calcium concentration from field-collected water data. Increased water hardness and alkalinity are characteristics of areas with high calcium concentrations, which are commonly found in areas with limestone or agricultural runoff that has been treated with lime (Ram et al., 2021). Regions with lower calcium levels, on the other hand, may have softer water as a result of distinct geological characteristics or less human interference. Mapping these variations is crucial for effective water resource management, ensuring appropriate treatment for domestic use, and maintaining ecological health. This targeted approach allows for precise interventions, such as adjusting agricultural practices or enhancing water treatment processes, to address specific calcium-related water quality issues. The higher concentration is represented in the blue color primarily in Khodu. whereas, the remaining part of the study area had less calcium concentration (97%) (Fig. 4 h).

#### 4.5.9. Total soluble solids

The spatial variation of total soluble solids (TSS) from field-collected water data reveals differences in the concentration of dissolved substances, such as minerals, salts, and organic matter, across various sampling locations. Areas with high TSS concentrations often indicate increased levels of dissolved minerals and salts, which can result from natural processes like mineral leaching from soil and rocks, as well as anthropogenic activities such as agricultural runoff, industrial discharge, and urban wastewater (Anyango et al., 2024). Elevated TSS levels can impact water quality by contributing to issues like hardness, salinity, and potential toxicity. Conversely, regions with lower TSS concentrations suggest purer water with fewer dissolved substances, indicating lesser human impact or natural dilution processes. Mapping these variations is crucial for water resource management, helping identify areas requiring intervention, such as improved wastewater treatment, sustainable agricultural practices, or protection of natural water sources to maintain optimal water quality for various uses. The northwestern, central, and southern part represented in dark red colour illustrates very high TSS concentrations in the range of 1500–4600, whereas, the remaining parts had TSS concentrations with a range of 180–500 meq/L represented in greenish blue color (Fig. 4 i).

#### 4.5.10. Sodium concentration

Differences in salinity across different sample sites, influenced by both natural and human-made factors, are shown by the geographical variation of sodium content in field-collected water data. The entry of saltwater, the discharge of road salt, or the use of sodium-based fertilizers in agriculture are the usual causes of locations with high sodium concentrations. Rising levels of sodium can deteriorate water quality,

which may harm human health and reduce agricultural productivity due to the risk of soil salinization. Conversely, areas with lower sodium concentrations generally experience less impact from these sources, indicating better water quality for irrigation. (Ram et al., 2021). Mapping these spatial variations is essential for targeted water management, enabling precise interventions to mitigate sodium pollution, protect water resources, and ensure the safety and suitability of water for various uses, including drinking, agriculture, and industrial processes. The northwestern, central, and southern part represented in blue color illustrates very high sodium concentrations in the range of 500–1100 meq/L whereas, the remaining parts had low sodium concentrations with a range of 1–100 meq/L represented in red color (Fig. 4 j)

#### 4.6. Sodium percentage

Significant regional variation was found across the research area when the location-specific distribution of sodium percentage was analyzed using data gathered in the field. Areas marked by a variety of human-caused processes, including urbanization, industrialization, and intensive agriculture operations, had notably elevated salt percentages. It is probable that irrigation with salt water or the use of fertilizers containing sodium contributed to the elevated soil sodium concentrations seen in these regions. Sodium percentages were found to be lower in less developed or natural locations, suggesting that there is less human impact and that the soil is healthier. These differences were clearly seen on the geographical maps made from the field data, which shed light on how human activities have affected soil salt levels. Fig. 5 shows that the sodium percentage is highest in the northwest and middle to southern regions of the research area, and lowest in the northern corner. Soil health dynamics and agricultural activities may be better understood with the help of this extensive geographical study.

#### 4.7. Sodium absorption ratio (SAR)

The analysis of spatial distribution for SAR, derived from field-collected data, revealed distinct patterns across the study area. Elevated SAR values were notably concentrated in certain regions, particularly those influenced by factors such as irrigation practices, soil composition, and geological characteristics (Panagos et al., 2012). These areas exhibited higher SAR values in the soil, indicative of potential salinity issues that could affect crop productivity and soil health. Conversely, lower SAR values were typically observed in less affected or natural areas, suggesting healthier soil conditions. The spatial maps generated from field data effectively depicted these variations, providing valuable insights into the potential impacts of SAR on agricultural land and groundwater quality. The central part of the study area represents a very high SAR whereas the remaining part illustrates a low to medium SAR (Fig. 6). This comprehensive spatial analysis contributes to our understanding of soil salinity dynamics and irrigation management practices.

#### 4.8. Permeability index

Results from the geographical analysis of PI, which were based on data obtained in the field, showed that there were substantial regional differences. Locations with naturally vegetated cover, low levels of human interference, and well-drained soils tended to have higher PI values, which indicate improved soil permeability. In contrast, locations characterized by urbanization, intense agricultural operations, and compacted soils showed lower PI values. This might be because these factors limit water penetration and increase runoff, as shown by Zhang et al. (2008). Decisions about land use, irrigation, and soil conservation may be better informed by these spatial patterns, which can be seen using geographic information system mapping, and which in turn shed light on hydrological processes and soil quality. Understanding the spatial distribution of PI is crucial for sustainable land management and

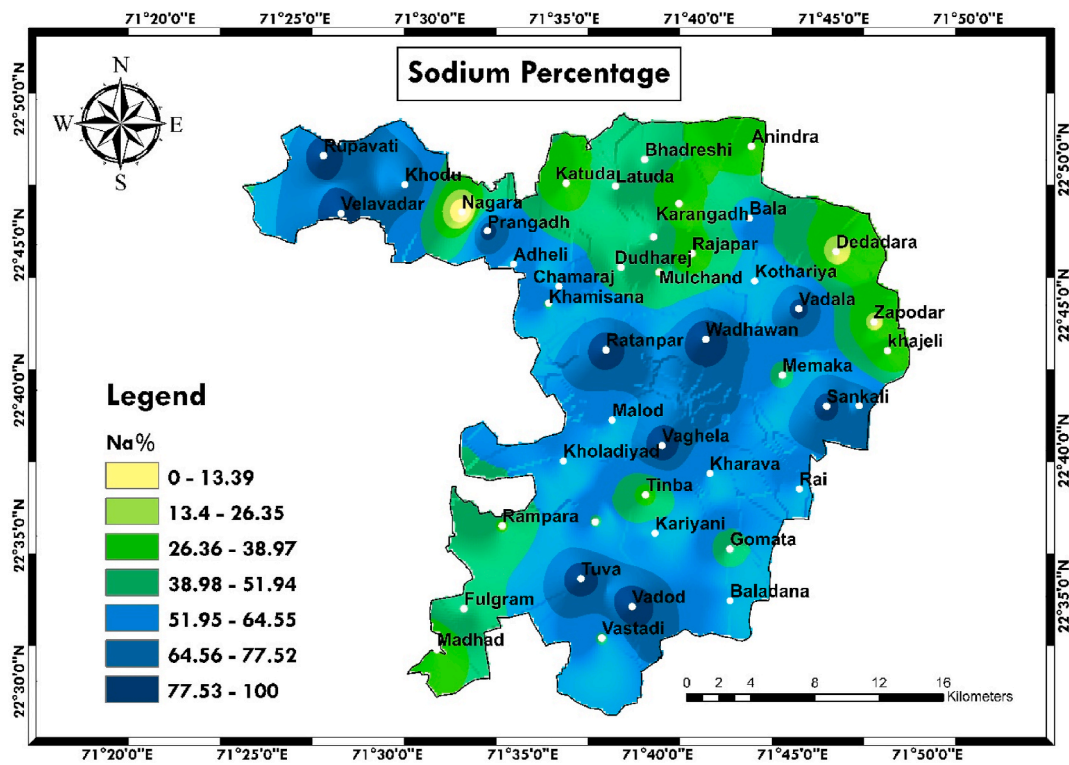


Fig. 5. Geographical Variation in Sodium Percentage across the study area.

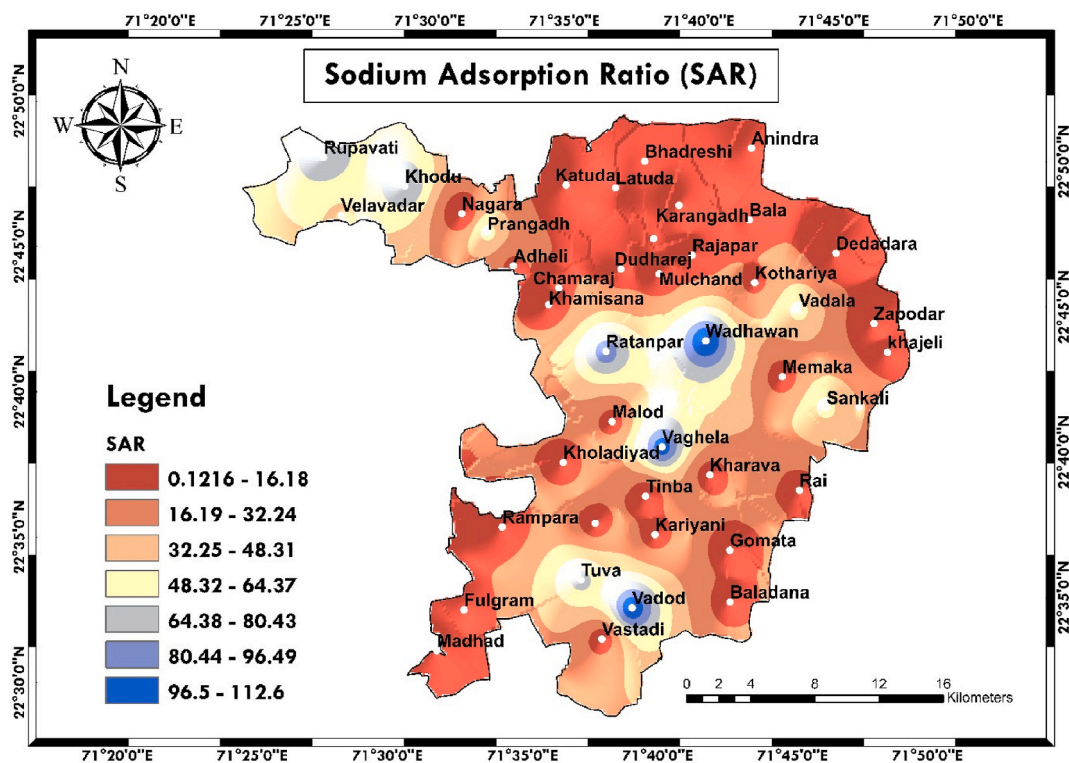


Fig. 6. Spatial Map of variation in sodium absorption ratio at different locations of the study area.

water resource protection, particularly in regions vulnerable to soil erosion, groundwater depletion, and flooding. The north-western region and central to the southern region of the study area represent a very high permeability index whereas the northern corner illustrates the less permeability index (Fig. 7).

#### 4.9. Irrigation Water Quality Index (IWQI)

It is one of the most efficient and commonly used methods for the evaluation of irrigation water quality for both stakeholders and policy-makers (Olusola Falowo 2017; Adimalla et al., 2020). The authors

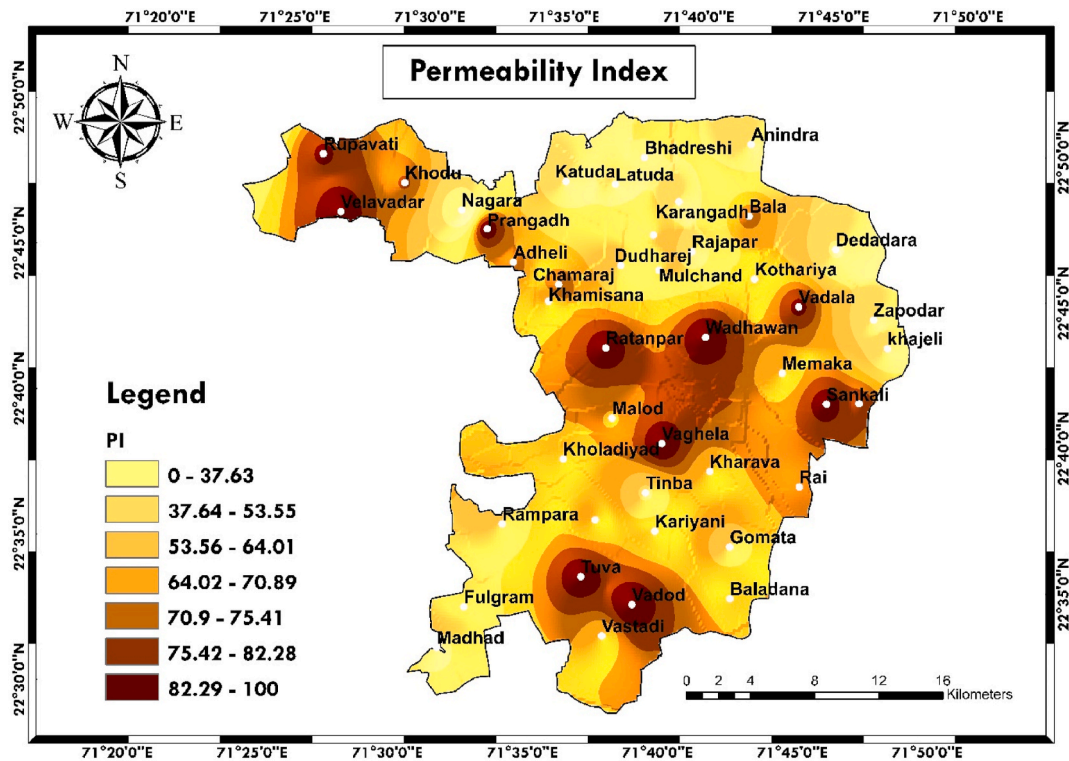


Fig. 7. Spatial Distribution of permeability index for the available soil across the study area.

provided a unique classification of irrigation water quality, focusing on its impact on soil and potential toxicity to crops and plants. The IWQI classification was based on five classes such as no restriction having IWQI range between 85 and 100, low restriction with the range 70–85, moderate restriction falling in the scale of 55–70, high restriction having IWQI values between 40 and 55, and lastly, severe restriction comprising of values within the IWQI range of 0–40 (Meireles et al., 2010; Khalaf and Hassan 2013; Abbasnia et al., 2018). The results of IWQI suggest that around 29% of the collected field data from different villages were found in the severe range (IWQI = 0–40) as illustrated in Table 3.

#### 4.10. Groundwater quality assessment

According to the IWQI findings for groundwater, about half of the field data obtained from several communities fell into the severe category (IWQI = 0–40). Furthermore, with an IWQI score of 40–55, about half of the 44 communities fell into the high restriction group. There was no indication that any of the towns fell into the categories of low limitation (IWQI = 70–85), no restriction (IWQI = 85–100), or moderate restriction (IWQI = 55–70) (Fig. 8, Table 4).

#### 4.11. Surface water quality assessment

The IWQI results for surface water show that around 17.85% of the field data collected from diverse localities fell into the severe category (IWQI = 0–40). Furthermore, about 60.71% of the 44 villages came into the group of high restriction (IWQI = 40–55). Only around 21.4% of municipalities fall into the moderate restriction category (IWQI = 55–70). Finally, none of the villages met the criteria for moderate limitation (IWQI = 70–85) or no restriction (IWQI = 85–100) (Fig. 9, Table 4).

#### 4.12. Water quality assessment

An examination of water samples obtained in the field using Piper

diagrams reveals different geochemical compositions and varieties of water (Ghazaryan et al., 2020). The ground water pipeline diagram displays a predominance of calcium and bicarbonate ions, suggesting a water type characterized by calcium bicarbonate. Conversely, the surface water piping diagram displays higher levels of sodium, chloride, and sulphate ions, suggesting a water type characterized by sodium chloride. The data suggest that many hydrogeochemical processes have an impact on the water chemistry in the research area. This might have implications for evaluating water quality and making decisions about resource management (see Fig. 10). Fig. 11 illustrates the quality of both surface and subterranean water, using a scale that spans from extremely poor (low) to exceptional (high).

#### 4.13. Recommendations

Validation of water quality tests for pond wells, tube wells, canal water, and bore wells by direct observation ground truthing is critical to ensure accuracy. Water samples were obtained from diverse sources, with a focus on varied depths and locations, so order to capture variability and estimate different parameters. Poor water quality had a negative impact on agriculture. Mango, lemon, and cumin output was considerably decreased due to poor water quality, as were vegetables and fruits such as brinjal, capsicum, and watermelon. After conducting the study, the following suggestions were made.

- It is acceptable to vary the irrigation technique based on the quality of the water used for irrigation. Instead of the conventional approach, it is recommended to utilize micro irrigation methods such as drip irrigation or sprinkler irrigation.
- Less tillage and cover crops are indications of improved soil management methods that lessen the impact of erosion and sedimentation, leading to cleaner, better water.
- Rigorous water quality monitoring programs are crucial for early detection of contaminants, complemented by effective treatment technologies like filtration and oxidation to ensure water meets irrigation standards.

**Table 3**

Demonstrates the physio-chemical parameters and IWQI calculated values.

Sr No.	Village	Source of water	HCO <sub>3</sub>	Cl (meq/L)	SAR (meq/L) <sup>1/2</sup>	Na+ (meq/L)	EC (µmho/cm)	Si-HCO <sub>3</sub>	Si-Cl	Si-SAR	Si-Na	Si-EC	IWQI
1	Khodu	Groundwater	176	3041	78.54	1027	8810	4.20	0.00	2.25	0.00	0.00	6.44
2	Dedadara	Pond	90	92	2.75	14	990	7.42	8.55	16.32	9.57	11.39	53.25
3	Tinba	Pond	100	78	4.18	18	990	7.25	8.58	14.20	9.55	11.39	50.97
4	Memaka	Groundwater	140	92	7.76	32	930	6.58	8.55	9.95	9.45	16.67	51.20
5	Bhadiyad	Canal	157	525	32.41	189	3010	6.29	7.58	7.69	8.36	7.37	37.29
6	Rajapar	Canal	88	64	3.25	14	940	7.45	8.61	15.66	9.57	11.75	53.04
7	Rampara	Canal	85	121	5	20	940	7.50	8.48	12.92	9.53	11.75	50.18
8	Prangadh	Groundwater	214	724	53.07	268	3960	5.34	7.14	6.47	7.81	6.16	32.92
9	Katuda	Canal	99	135	3.17	14	920	7.27	8.45	15.80	9.57	16.74	57.83
10	Anindra	Canal	101	64	3.79	18	990	7.23	8.61	14.81	9.55	11.39	51.60
11	Tuva	Pond	353	554	69.3	392	3890	3.00	7.52	5.52	6.95	6.25	29.24
12	Madhad	Groundwater	140	71	3.3	14	980	6.58	8.59	15.59	9.57	11.46	51.80
13	Mulchand	Canal	215	133	5.59	25	500	5.32	8.46	11.99	9.50	19.37	54.63
14	Velavadar	Ground water	285	753	47	235	3930	4.14	7.07	6.83	8.04	6.20	32.28
15	Latuda	Canal	29	226	10.45	64	1000	8.44	8.25	7.83	9.23	16.18	49.93
16	Bhadreshi	Canal	105	104	7	35	660	7.17	8.52	10.55	9.43	18.45	54.12
17	Kariyani	Groundwater	84	89	10.23	44	510	7.52	8.55	8.01	9.37	19.32	52.76
18	khajeli	Canal	56	158	3.53	16	300	7.99	8.40	15.22	9.56	20.52	61.70
19	Vadod	Groundwater	353	745	109.93	655	3500	3.00	7.09	3.14	5.12	6.75	25.09
20	Chamaraj	Canal	132	143	15.37	67	800	6.71	8.43	8.69	9.21	17.58	50.62
21	Vaghela	Groundwater	338	766	105.56	655	3700	3.25	7.04	3.39	5.12	6.50	25.30
22	Vadala	Canal	132	575	52.44	308	2600	6.71	7.47	6.51	7.53	8.79	37.01
23	Bala	Canal	117	86	11.36	44	600	6.96	8.56	7.12	9.37	18.80	50.81
24	Dudharej	Canal	134	229	11.52	71	1000	6.68	8.24	6.99	9.18	16.18	47.27
25	Kholadiyad	Canal	138	92	9.53	41	500	6.61	8.55	8.56	9.39	19.37	52.48
26	Kharava	Canal	115	173	9.66	41	520	7.00	8.37	8.45	9.39	19.26	52.46
27	Karangadh	Canal	126	219	3.88	18	440	6.81	8.26	14.68	9.55	19.72	59.02
28	Kothariya	Canal	153	129	13.14	67	720	6.36	8.46	8.82	9.21	18.11	50.95
29	Gundiya	Pond	121	75	8.96	38	5250	6.90	8.58	9.01	9.41	4.53	38.43
30	Sankali	Groundwater	303	289	53.11	286	2000	3.84	8.11	6.47	7.68	10.90	37.00
31	Ratanpar	Groundwater	421	743	89.29	599	3620	1.86	7.09	4.35	5.51	6.60	25.40
32	Adheli	Canal	131	141	13.59	60	700	6.73	8.44	8.79	9.25	18.22	51.43
33	Rupavati	Groundwater	154	1263	76.66	655	4300	6.34	5.93	5.09	5.12	5.73	28.21
34	Gomata	Groundwater	102	128	9.81	50	600	7.22	8.47	8.34	9.32	18.80	52.15
35	Nagara	Groundwater	287	1602	0.12	1	5900	4.11	5.18	18.41	9.66	3.70	41.05
36	Wadhawan	Canal	275	790	112.74	713	3900	4.31	6.99	2.97	4.71	6.24	25.23
37	Vastadi	Groundwater	90	70	8.13	32	400	7.42	8.60	9.66	9.45	19.95	55.08
38	Bakarthali	Canal	89	127	9.17	44	600	7.44	8.47	8.84	9.37	18.80	52.91
39	Khamisana	Ground water	79	53	7.49	27	300	7.60	8.63	10.17	9.48	20.52	56.41
40	Fulgram	Ground water	87	80	8.74	41	520	7.47	8.57	9.18	9.39	19.26	53.87
41	Baladana	Canal	178	89	10.23	44	850	5.94	8.55	8.01	9.37	17.23	49.10
42	Malod	Pond	99	76	9.81	38	540	7.27	8.58	8.34	9.41	19.14	52.74
43	Zapodar	Canal	83	29	2.63	11	300	7.54	8.69	16.19	9.59	20.52	62.53
44	Rai	Pond	94	70	9.71	35	510	7.35	8.60	8.42	9.43	19.32	53.11

- Ensure proper drainage to prevent waterlogging and salt deposition.
- Artificial recharge to augment the natural recharge process and improve water quality.
- Selection of crop:
  - The main crops grown in Surendranagar, an agricultural area, are cumin and cotton. Some other important crops include peanuts, millet, wheat, and sesame. On average, small farmers possess 1.22 ha of land, which accounts for almost 37% of the total.
  - Based on the water quality, the suggested crops for the Rabi season are wheat, barley, cumin, peas, grams, and mustard. For the kharif season, the crops to grow are cotton, sugarcane, jowar, bajra, maize, and bajra.

#### 4.14. Irrigation water quality related to Sustainable Development Goals (SDGs)

Irrigation water quality plays a crucial role in achieving several Sustainable Development Goals (SDGs), making it a cornerstone of sustainable agriculture and environmental stewardship. SDG 2 (Zero Hunger) is directly impacted by irrigation water quality as it ensures healthy crop growth, essential for food security and increasing agricultural productivity. High-quality water is essential for sustainable food production and resilient agricultural practices, which are crucial for

achieving the targets of SDG 2 (Omar et al., 2020). Water quality is addressed under SDG 6 (Clean Water and Sanitation) via prioritizing the elimination of pollution and increasing water-use efficiency. Water supplies can be safeguarded from pollution and sustainable water management techniques can be advanced by continuing to uphold stringent regulations for irrigation water. The importance of irrigation water quality extends to SDG 15 (Life on Land), which encourages the protection and sustainable use of terrestrial and freshwater ecosystems. Good water quality reduces soil deterioration and encourages biodiversity, resulting in sustainable land use (Pe'er et al., 2020). Furthermore, the quality of irrigation water influences SDG 3 (Good Health and Well-being) since polluted water may cause toxic compounds to accumulate in crops, presenting major health hazards when these products reach the food chain. Ensuring clean irrigation water helps reduce illnesses from hazardous chemicals, thus supporting SDG 3 (Lal 2012). SDG 12 (Responsible Consumption and Production) also emphasizes the need for environmentally sound management of chemicals and efficient use of natural resources. Furthermore, irrigation water quality is also pivotal for SDG 13 (Climate Action), as it helps build resilience in agricultural systems against climate-related hazards such as droughts and changing precipitation patterns. Ensuring high-quality water for irrigation contributes to adaptive capacity and mitigates the adverse effects of climate change (Bhattacharyya et al., 2015). Proper

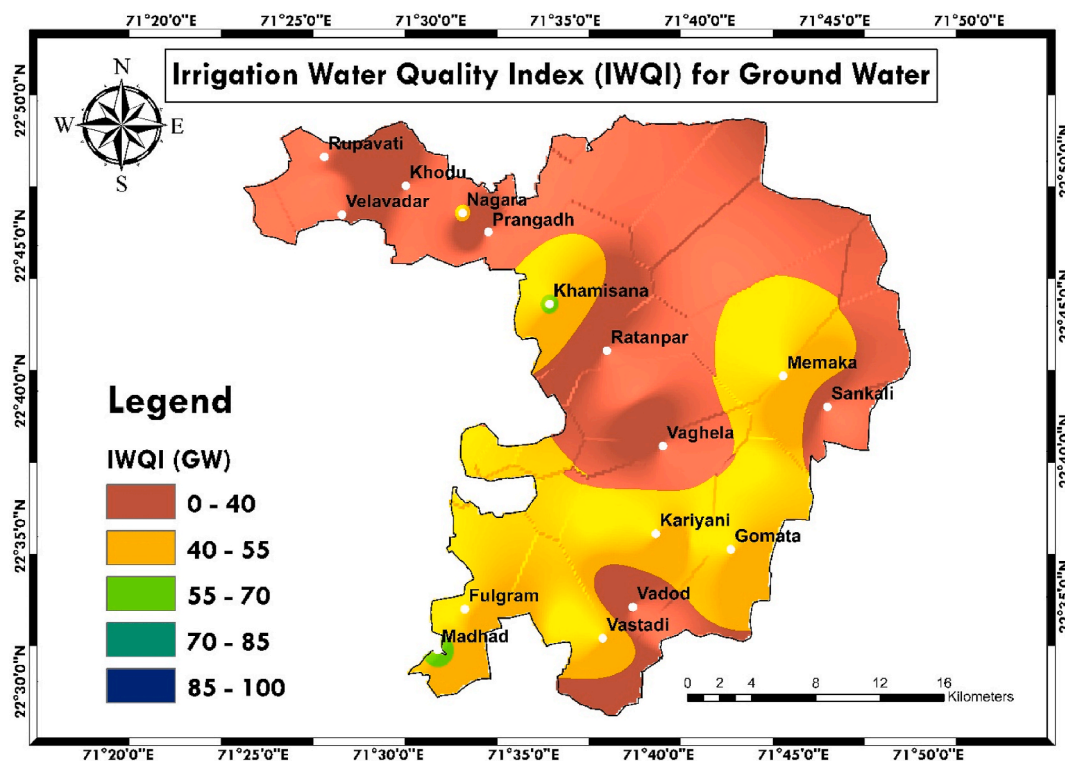


Fig. 8. The surface water quality classification using the Irrigation water quality Index.

Table 4

Illustrates the groundwater quality classification for the investigated villages based on IWQI.

Classification of Irrigation Water Quality Index (IWQI)				
IWQI values	Water use restriction	No. of samples	Percentage of samples	Sample number
85–100	No restriction	0	0	–
70–85	Low restriction	0	0	–
55–70	Moderate restriction	6	13.64	9, 18, 27, 37, 39, 43
40–55	High restriction	25	56.82	2, 3, 4, 6, 7, 10, 12, 13, 15, 16, 17, 20, 23, 24, 25, 26, 28, 32, 34, 35, 38, 40, 41, 42, 44
0–40	Severe restriction	13	29.54	1, 5, 8, 11, 14, 19, 21, 22, 29, 30, 31, 33, 36

management of irrigation water quality prevents the introduction of harmful substances into the environment, supporting responsible agricultural practices. Managing irrigation water quality helps prevent marine pollution, protect aquatic ecosystems, and support the health of marine life. To summarize, the quality of irrigation water is critical to attaining many SDGs since it supports sustainable farming practices, improves public health, conserves water resources, and preserves ecosystems on land and in water. Addressing irrigation water quality holistically helps accelerate progress toward these interrelated objectives, emphasizing the necessity of comprehensive water management techniques that are aligned with the larger sustainability agenda. Ensuring that irrigation water meets high standards benefits not only food security and public health, but also the resilience and sustainability of our natural environment, emphasizing the interconnectedness of the SDGs and the critical role that water quality plays in achieving them. By concentrating on preserving and enhancing irrigation water quality, we can make substantial progress toward a more sustainable and equitable

future, aligning agricultural practices with the global goals established in the SDGs.

#### 4.15. Limitations and future scope

The present research includes limitations that may affect the accuracy and usefulness of the findings. Satellite imaging, such as Landsat and Sentinel II, may lack adequate spatial and temporal resolution to reliably detect small-scale variations in water quality and availability. This may result in errors when appraising particular sites. Furthermore, the accuracy of indices such as NDVI, NDWI, and LSWI may be influenced by atmospheric conditions and sensor limitations, jeopardizing the validity of water availability and quality assessments. The study's reliance on sample data may not adequately portray groundwater variability over the whole region, and variations in groundwater quality over time and at different levels may limit the results' application. The study provides an evaluation of current water quality, but it does not include anticipated changes in land use, climate, or water management strategies that may affect groundwater and surface water conditions in the future. To overcome these limitations, future research might benefit from a variety of enhancements. Higher-resolution satellite pictures or drone-based observations might improve the spatial precision of water quality measures. Furthermore, integrating real-time monitoring data with remote sensing might lead to a more comprehensive analysis of water quality and availability. Implementing longitudinal studies to monitor changes in water quality over time would help determine the impact of seasonal variations, climate change, and land use changes on water suitability. Expanding the IWQI to include other water quality metrics and soil properties, such as heavy metals, organic contaminants, and emerging pollutants, might give a more thorough assessment of irrigation water suitability. Using contemporary hydrological models to simulate different scenarios for water extraction, land use changes, and climate consequences might provide important insights into sustainable water management techniques. Creating user-friendly decision support systems using IWQI and GIS data might assist farmers, regulators, and water resource managers make better decisions.

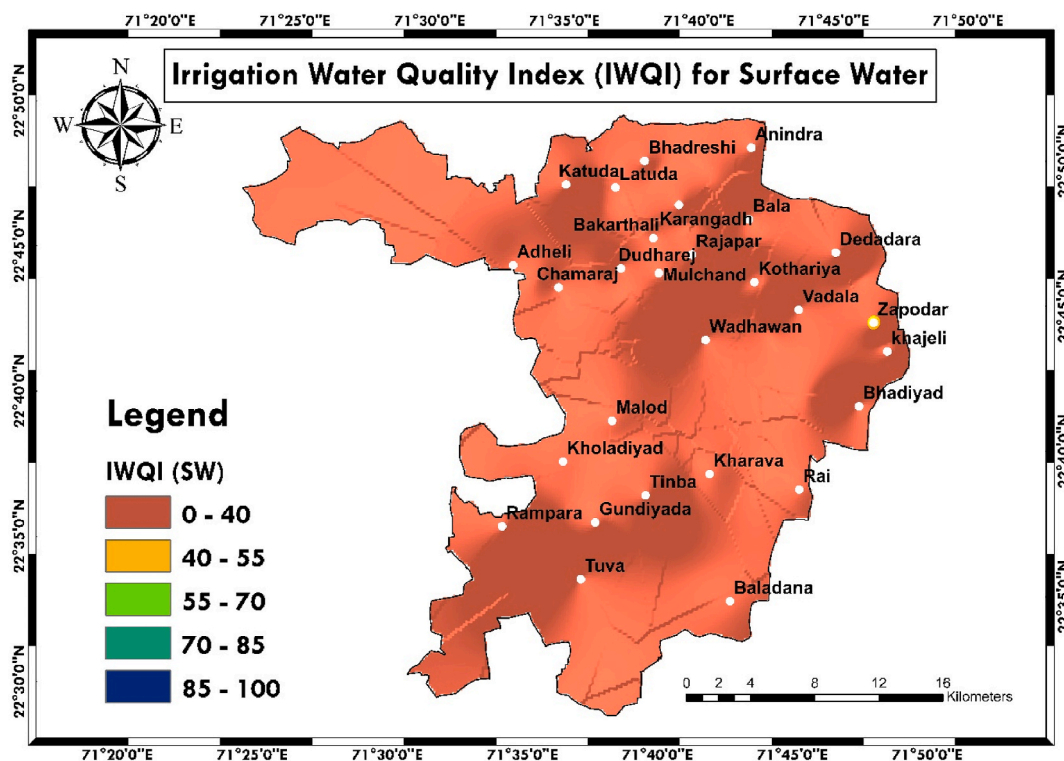


Fig. 9. The surface water quality classification using the Irrigation water quality Index.

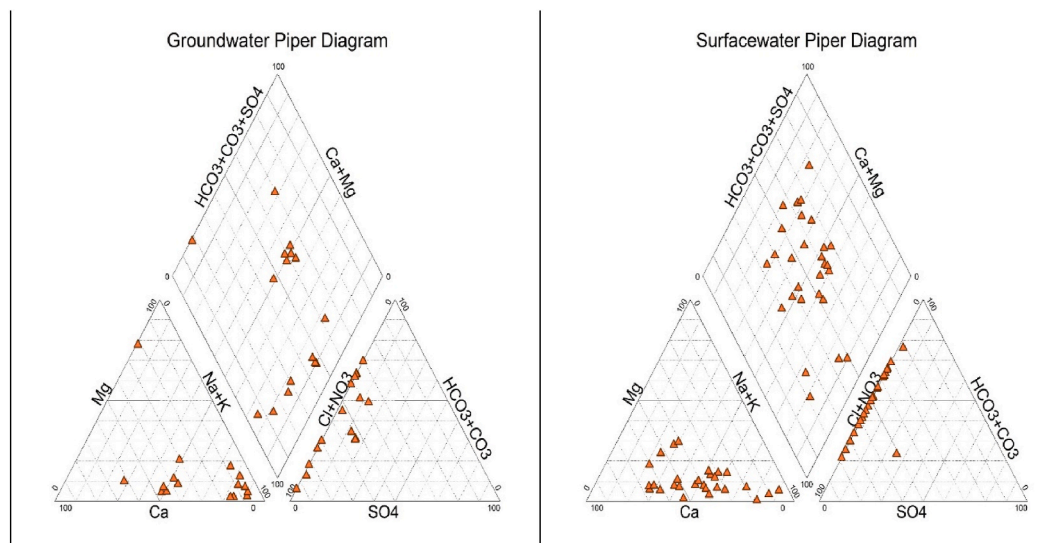


Fig. 10. Classification of groundwater and surface water quality according to Piper scheme.

**5. Conclusion**

This study underscores the urgent need for assessing groundwater quality to achieve sustainable irrigation in the Wadhwan region, Gujarat. By integrating the IWQI, GIS zoning maps, and satellite indices (NDVI, NDWI, LSWI), the research reveals significant water quality concerns, with nearly 50% of groundwater samples classified under severe restrictions (IWQI = 0–40) and the remaining largely under high restriction (IWQI = 40–55). Surface water analysis shows similar trends, highlighting widespread challenges across the region. The geospatial analysis further identifies specific areas like Rupavati and Khodu Velavadar with critically low water quality. Additionally, hydro-chemical facies indicate mixed water types dominated by Ca<sup>2+</sup>-Mg<sup>2+</sup>-Cl<sup>-</sup> and

Na-HCO<sub>3</sub> classes. This research aligns with SDGs 2, 6, and 15, promoting better water management, sustainable agriculture, and ecosystem conservation. The findings provide a comprehensive framework for future water resource management and agricultural planning in the region, emphasizing the need for immediate intervention to enhance irrigation suitability and ensure long-term sustainability.

**CRediT authorship contribution statement**

**Uttam Vyas:** Writing – review & editing, Writing – original draft, Software. **Dhruvesh Patel:** Writing – review & editing, Writing – original draft, Supervision, Software, Methodology, Conceptualization. **Vinay Vakharia:** Supervision. **Keval H. Jodhani:** Writing – review &

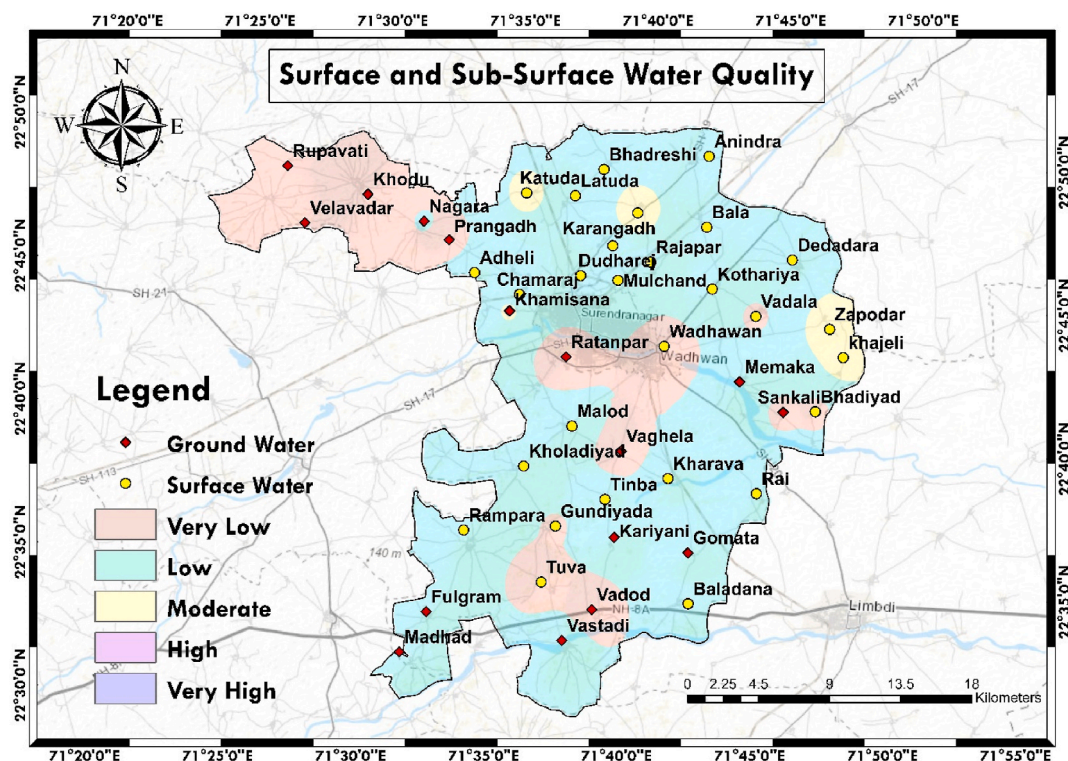


Fig. 11. Surface and Sub-surface water quality with a range of Very low (poor) to Very High (excellent).

editing, Writing – original draft, Software, Methodology, Investigation, Formal analysis, Conceptualization.

#### Declaration of competing interest

The authors declare that they have no known competing financial interests or personal relationships that could have appeared to influence the work reported in this paper.

#### Data availability

Data will be made available on request.

#### References

- Abbasnia, A., Radfard, M., Mahvi, A.H., Nabizadeh, R., Yousefi, M., Soleimani, H., Alimohammadi, M., 2018. Groundwater quality assessment for irrigation purposes based on irrigation water quality index and its zoning with GIS in the villages of Chabahar, Sistan and Baluchistan, Iran. *Data Brief* 19, 623–631. <https://doi.org/10.1016/j.dib.2018.05.061>.
- Acharya, T., Subedi, A., Lee, D., 2018. Evaluation of water indices for surface water extraction in a Landsat 8 Scene of Nepal. *Sensors* 18 (8), 2580. <https://doi.org/10.3390/s18082580>.
- Acharya, S., Khandegar, V., Sharma, S.K., 2024. Groundwater Quality Assessment of Newly Developed Dwarka Region. In: *Journal of Hazardous, Toxic, and Radioactive Waste*, Vol. 28, Issue 2. American Society of Civil Engineers (ASCE, New Delhi, India. <https://doi.org/10.1061/jhtrbp.hzeng-1265>.
- Acharya, T.D., Subedi, A., Huang, H., Lee, D.H., 2019. Application of water indices in surface water change detection using Landsat imagery in Nepal. *Sensor. Mater.* 31 (5), 1429. <https://doi.org/10.18494/SAM.2019.2264>.
- Adimalla, N., Dhakate, R., Kasarla, A., Taloor, A.K., 2020. Appraisal of groundwater quality for drinking and irrigation purposes in Central Telangana, India. *Groundwater for Sustainable Development* 10, 100334. <https://doi.org/10.1016/j.gsd.2020.100334>.
- Albarqouni, M.M.Y., Yagmur, N., Bektas Balcik, F., Sekertekin, A., 2022. Assessment of spatio-temporal changes in water surface extents and lake surface temperatures using google earth engine for lakes region, Türkiye. *ISPRS Int. J. Geo-Inf.* 11 (7), 407. <https://doi.org/10.3390/ijgi11070407>.
- Anyango, G.W., Bhowmick, G.D., Sahoo Bhattacharya, N., 2024. A critical review of irrigation water quality index and water quality management practices in micro-irrigation for efficient policy making. *Desalination Water Treat.* 318, 100304. <https://doi.org/10.1016/j.dwt.2024.100304>.
- Batarseh, M., et al., 2021. Assessment of groundwater quality for irrigation in the arid regions using irrigation water quality index (IWQI) and GIS-Zoning maps: case study from Abu Dhabi Emirate, UAE. *Groundwater for Sustainable Development* 14, 100611. <https://doi.org/10.1016/j.gsd.2021.100611>.
- Bhattacharyya, R., et al., 2015. Soil degradation in India: challenges and potential solutions. *Sustainability* 7 (4), 3528–3570. <https://doi.org/10.3390/su7043528>.
- Cruz-Montes, E.E., Durango-Banquett, M.M., Torres-Bejarano, F.M., Campo-Daza, G.A., Padilla-Mendoza, C., 2023. Remote sensing application using Landsat 8 images for water quality assessments. *J. Phys. Conf.* 2475 (1), 012007. <https://doi.org/10.1088/1742-6596/2475/1/012007>.
- Dervisoglu, A., 2021. Analysis of the temporal changes of inland Ramsar sites in Turkey using google earth engine. *ISPRS Int. J. Geo-Inf.* 10 (8), 521. <https://doi.org/10.3390/ijgi10080521>.
- Doneen, L.D., 1964. *Notes on water quality in agriculture*. Department of Water Sciences and Engineering. University of California, Davis. *Water Science and Engineering. Paper 4001*.
- El-Amier, Y.A., Kotb, W.K., Bonanomi, G., Fakhry, H., Marraiki, N.A., Abd-ElGawad, A. M., 2021. Hydrochemical assessment of the irrigation water quality of the El-Salam canal, Egypt. *Water* 13 (17), 2428. <https://doi.org/10.3390/w13172428>.
- Feng, Z., et al., 2023. Analysis of water quality indexes and their relationships with vegetation using self-organizing map and geographically and temporally weighted regression. *Environ. Res.* 216, 114587. <https://doi.org/10.1016/j.envres.2022.114587>.
- Gond, S., Gupta, N., Dikshit, P.K.S., Patel, J., 2023a. Assessment of drought variability using SPEI under observed and projected climate scenarios over Uttar Pradesh, India. *Phys. Chem. Earth, Parts A/B/C* 131, 103440. <https://doi.org/10.1016/j.pce.2023.103440>.
- Gond, S., Gupta, N., Patel, J., Dikshit, P.K.S., 2023b. Spatiotemporal evaluation of drought characteristics based on standard drought indices at various timescales over Uttar Pradesh, India. *Environ. Monit. Assess.* 195 (3), 439. <https://doi.org/10.1007/s10661-023-10988-2>.
- Gujrati, A., Jha, V.B., 2018. Surface water dynamics OF inland water bodies of India using google earth engine. *ISPRS Annals of the Photogrammetry, Remote Sensing and Spatial Information Sciences IV-5*, 467–472. <https://doi.org/10.5194/isprs-annals-IV-5-467-2018>.
- Gupta, N., Banerjee, A., Gupta, S.K., 2021. Spatio-temporal trend analysis of climatic variables over Jharkhand, India. *Earth Systems and Environment* 5 (1), 71–86. <https://doi.org/10.1007/s41748-021-00204-x>.
- Gupta, N., Gond, S., Gupta, S.K., 2022. Spatiotemporal trend characteristics of rainfall and drought jeopardy over Bundelkhand Region, India. *Arabian J. Geosci.* 15 (12), 1155. <https://doi.org/10.1007/s12517-022-10389-8>.
- Hussein, E.E., et al., 2024. Groundwater quality assessment and irrigation water quality index prediction using machine learning algorithms. *Water* 16 (2), 264. <https://doi.org/10.3390/w16020264>.
- Hussein, N.M., Assaf, M.N., 2020. Multispectral remote sensing utilization for monitoring chlorophyll-a levels in inland water bodies in Jordan. *Sci. World J.* 2020, 1–14. <https://doi.org/10.1155/2020/5060969>.



- Jodhani, K., Bansal, P., Jain, P., 2021. Shoreline Change and Rate Analysis of Gulf of Khambhat Using Satellite Images, pp. 151–170. [https://doi.org/10.1007/978-981-16-1303-6\\_12](https://doi.org/10.1007/978-981-16-1303-6_12).
- Jodhani, K.H., et al., 2024a. Assessment of forest fire severity and land surface temperature using Google Earth Engine: a case study of Gujarat State, India. *Fire Ecology* 20 (1), 23. <https://doi.org/10.1186/s42408-024-00254-2>.
- Jodhani, K.H., et al., 2024b. Synergizing google earth engine and earth observations for potential impact of land use land cover on air quality. *Results in Engineering*, 102039. <https://doi.org/10.1016/j.rineng.2024.102039>.
- Jodhani, K.H., et al., 2024c. Unveiling seasonal fluctuations in air quality using google earth engine: a case study for Gujarat, India. *Top. Catal.* <https://doi.org/10.1007/s11244-024-01957-1>.
- Jodhani, K.H., Patel, D., Madhavan, N., Gupta, N., Singh, S.K., Rathnayake, U., 2024d. Unravelling flood risk in the Rel River Watershed, Gujarat using coupled earth observations, multi criteria decision making and google earth engine. In: *Results in Engineering*. Elsevier BV, p. 102836. <https://doi.org/10.1016/j.rineng.2024.102836>.
- Jodhani, K.H., Jodhani, K.H., Patel, D., Madhavan, N., 2023a. Land use land cover classification for REL river using machine learning techniques. In: 2023 International Conference on IoT, Communication and Automation Technology (ICICAT). IEEE, pp. 1–3. <https://doi.org/10.1109/ICICAT57735.2023.10263663>.
- Jodhani, K.H., Patel, D., Madhavan, N., 2023b. A review on analysis of flood modelling using different numerical models. *Mater. Today: Proc.* 80, 3867–3876. <https://doi.org/10.1016/j.matpr.2021.07.405>.
- Jodhani, K.H., Patel, D., Madhavan, N., Singh, S.K., 2023c. Soil erosion assessment by RUSLE, google earth engine, and geospatial techniques over rel river watershed, Gujarat, India. *Water Conservation Science and Engineering* 8 (1), 49. <https://doi.org/10.1007/s41101-023-00223-x>.
- Jodhani, K.H., Patel, D., Madhavan, N., Soni, U., Patel, H., Singh, S.K., 2024e. Channel planform dynamics using earth observations across Rel river, western India: a synergetic approach. *Spatial Information Research*. <https://doi.org/10.1007/s41324-024-00573-1>.
- Kaplan, G., Avdan, Z.Y., Goncu, S., Avdan, U., 2019. Evaluation of RapidEye-3 satellite data for assessing water turbidity of lake Borabey. In: *The 4th International Electronic Conference on Water Sciences*. MDPI, Basel Switzerland, p. 14. <https://doi.org/10.3390/ECWS-4-06424>.
- Karmakar, B., Singh, M.K., Choudhary, B.K., Singh, S.K., Egbueri, J.C., Gautam, S.K., Rawat, K.S., 2023. Investigation of the hydrogeochemistry, groundwater quality, and associated health risks in industrialized regions of Tripura, northeast India. *Environ. Forensics* 24 (5–6), 285–306. <https://doi.org/10.1080/15275922.2021.2006363>.
- Khalaf, R.M., Hassan, W.H., 2013. EVALUATION OF IRRIGATION WATER QUALITY INDEX (IWQI) FOR AL-DAMMAM CONFINED AQUIFER IN THE WEST AND SOUTHWEST OF KARBALA CITY, IRAQ, pp. 21–34.
- Khan, R.M., Salehi, B., Mahdianpari, M., Mohammadimanesh, F., 2021. Water quality monitoring over FINGER lakes region using SENTINEL-2 imagery on google earth engine cloud computing platform. *ISPRS Annals of the Photogrammetry, Remote Sensing and Spatial Information Sciences* V-3–2021, 279–283. <https://doi.org/10.5194/isprs-annals-v-3-2021-279-2021>.
- Khaniya, B., Gunathilake, M.B., Rathnayake, U., 2021. Ecosystem-based adaptation for the impact of climate change and variation in the water management sector of Sri Lanka. *Math. Probl. Eng.* 2021, 1–10. <https://doi.org/10.1155/2021/8821329>.
- Kumar, N., Singh, S.K., 2021. Soil erosion assessment using earth observation data in a trans-boundary river basin. *Nat. Hazards* 107 (1), 1–34. <https://doi.org/10.1007/s11069-021-04571-6>.
- Kumar Pradhan, R., Srivastava, P.K., Maurya, S., Kumar Singh, S., Patel, D.P., 2020. Integrated framework for soil and water conservation in Kosi River Basin. *Geocarto Int.* 35 (4), 391–410. <https://doi.org/10.1080/10106049.2018.1520921>.
- Lal, R., 2012. Climate change and soil degradation mitigation by sustainable management of soils and other natural resources. *Agric. Res.* 1 (3), 199–212. <https://doi.org/10.1007/s40003-012-0031-9>.
- Liuzzo, L., Puleo, V., Nizza, S., Freni, G., 2020. Parameterization of a bayesian normalized difference water index for surface water detection. *Geosciences* 10 (7), 260. <https://doi.org/10.3390/geosciences10070260>.
- Makubura, R., Meddage, D.P.P., Azamathulla, H.Md, Pandey, M., Rathnayake, U., 2022. A simplified mathematical formulation for water quality index (wqi): a case study in the kelani river basin, Sri Lanka. *Fluid* 7 (5), 147. <https://doi.org/10.3390/fluids7050147>.
- Maliqi, E., Jusufi, K., Singh, S.K., 2020. Assessment and spatial mapping of groundwater quality parameters using metal pollution indices, graphical methods and Geoinformatics. *Analytical Chemistry Letters* 10 (2), 152–180. <https://doi.org/10.1080/22297928.2020.1764384>.
- Maliqi, E., Kumar, N., Latifi, L., Singh, S., 2023. Soil erosion estimation using an Empirical model, hypsometric integral and geo-information science – a case study. *Ecological Engineering & Environmental Technology* 24 (4), 62–72. <https://doi.org/10.12912/27197050/161957>.
- Meireles, A.C.M., Andrade, E.M. de, Chaves, L.C.G., Frischkorn, H., Crisostomo, L.A., 2010. A new proposal of the classification of irrigation water. *Rev. Cienc. Agron.* 41 (3), 349–357. <https://doi.org/10.1590/S1806-66902010000300005>.
- Mohd Nazri, N.A., Ismain, S.H.A., Foronda, V., Salleh, S.A., Abdullah, M.F., 2024. Spatio temporal analysis of water quality at tasek Bera. *IOP Conf. Ser. Earth Environ. Sci.* 1316 (1), 012004 <https://doi.org/10.1088/1755-1315/1316/1/012004>.
- Nemčić-Jurec, J., Singh, S.K., Jazbec, A., Gautam, S.K., Kovač, I., 2019. Hydrochemical investigations of groundwater quality for drinking and irrigational purposes: two case studies of Koprivnica-Krizevci County (Croatia) and district Allahabad (India). *Sustainable Water Resources Management* 5 (2), 467–490. <https://doi.org/10.1007/s40899-017-0200-x>.
- Odermatt, D., Danne, O., Philipson, P., Brockmann, C., 2018. Diversity II water quality parameters from ENVISAT (2002–2012): a new global information source for lakes. *Earth Syst. Sci. Data* 10 (3), 1527–1549. <https://doi.org/10.5194/essd-10-1527-2018>.
- Olusola Falowo, O., 2017. Irrigation and drinking water quality index determination for groundwater quality evaluation in akoko northwest and northeast areas of Ondo state, Southwestern Nigeria. *American Journal of Water Science and Engineering* 3 (5), 50. <https://doi.org/10.11648/j.ajwse.20170305.11>.
- Omar, D., Idrees, M., Ahmadu, H., Yusuf, A., Ipadeola, O., Babalola, A., Abdulyekeen, A., 2022. Assessment of vegetation dynamics and forest loss using google earth engine and multi-temporal sentinel-2 imagery. *Agro-Science* 21 (2), 85–94. <https://doi.org/10.4314/as.v21i2.10>.
- Omar, P.J., Dwivedi, S.B., Dikshit, P.K.S., 2020. Sustainable Development and Management of Groundwater in Varanasi, India, pp. 201–209. [https://doi.org/10.1007/978-981-13-8181-2\\_15](https://doi.org/10.1007/978-981-13-8181-2_15).
- Panagos, P., Karydas, C.G., Gitas, I.Z., Montanarella, L., 2012. Monthly soil erosion monitoring based on remotely sensed biophysical parameters: a case study in Strymonas river basin towards a functional pan-European service. *International Journal of Digital Earth* 5 (6), 461–487. <https://doi.org/10.1080/17538947.2011.587897>.
- Qadir, M., et al., 2018. High-magnesium waters and soils: emerging environmental and food security constraints. *Sci. Total Environ.* 642, 1108–1117. <https://doi.org/10.1016/j.scitotenv.2018.06.090>.
- Quinn, N.W.T., et al., 2022. Applications of GIS and remote sensing in public participation and stakeholder engagement for watershed management. *Socio-Environmental Systems Modelling* 4, 18149. <https://doi.org/10.18174/semso.18149>.
- Ram, A., Tiwari, S.K., Pandey, H.K., Chaurasia, A.K., Singh, S., Singh, Y.V., 2021. Groundwater quality assessment using water quality index (WQI) under GIS framework. *Appl. Water Sci.* 11 (2), 46. <https://doi.org/10.1007/s13201-021-01376-7>.
- Rawat, K., Pradhan, S., Tripathi, V., Jeyakumar, L., Singh, S.K., 2019. Statistical approach to evaluate groundwater contamination for drinking and irrigation suitability. *Groundwater for Sustainable Development* 9, 100251. <https://doi.org/10.1016/j.gsd.2019.100251>.
- Rawat, K.S., Singh, S.K., 2018. Appraisal of soil conservation capacity using NDVI model-based C factor of RUSLE model for a semi arid ungauged watershed: a case study. *Water Conservation Science and Engineering* 3 (1), 47–58. <https://doi.org/10.1007/s41101-018-0042-x>.
- Rawat, K.S., Singh, S.K., Gautam, S.K., 2018a. Assessment of groundwater quality for irrigation use: a peninsular case study. *Appl. Water Sci.* 8 (8), 233. <https://doi.org/10.1007/s13201-018-0866-8>.
- Rawat, K.S., Singh, S.K., Gautam, S.K., 2018b. Assessment of groundwater quality for irrigation use: a peninsular case study. *Appl. Water Sci.* 8 (8), 233. <https://doi.org/10.1007/s13201-018-0866-8>.
- Rekha, V.B., Thomas, A.P., Suma, M., Vijith, H., 2011. An integration of spatial information technology for groundwater potential and quality investigations in koduvan Ar sub-watershed of Meenachil river basin, Kerala, India. *Journal of the Indian Society of Remote Sensing* 39 (1), 63–71. <https://doi.org/10.1007/s12524-010-0050-6>.
- Rokni, K., Ahmad, A., Selamat, A., Hazini, S., 2014. Water feature extraction and change detection using multitemporal Landsat imagery. *Rem. Sens.* 6 (5), 4173–4189. <https://doi.org/10.3390/rs6054173>.
- Sha, T., Yao, X., Wang, Y., Tian, Z., 2022. A quick detection of lake area changes and hazard assessment in the qinghai–Tibet plateau based on GEE: a case study of Tuosuo lake. *Front. Earth Sci.* 10 <https://doi.org/10.3389/feart.2022.934033>.
- Shil, S., Singh, U.K., Mehta, P., 2019. Water quality assessment of a tropical river using water quality index (WQI), multivariate statistical techniques and GIS. *Appl. Water Sci.* 9 (7), 168. <https://doi.org/10.1007/s13201-019-1045-2>.
- Shivhare, N., Omar, P.J., Gupta, N., Dikshit, P.K.S., 2016. Runoff estimation of Banaras Hindu University South Campus using ArcGIS and HecGeo-HMS. In: 2016 3rd International Conference on Recent Advances in Information Technology (RAIT). IEEE, pp. 607–612. <https://doi.org/10.1109/RAIT.2016.7507968>.
- Silva Filho, G.C., et al., 2020. Detecting spatiotemporal variability in the physicochemical properties of water in the Lower Mearim using remote sensing data. *Cienc. Nat.* 42, e32. <https://doi.org/10.5902/2179460X40984>.
- Singh, S.K., Bharose, R., Nemčić-Jurec, J., Rawat, K.S., Singh, D., 2021. Irrigation water quality appraisal using statistical methods and WATEQ4F geochemical model. In: *Agricultural Water Management*. Elsevier, pp. 101–138. <https://doi.org/10.1016/B978-0-12-812362-1.00007-2>.
- Solomon, A.O., Agada, I.S., Piwuna, R.M., Imagbe, L.O., Aga, T., Chup, A.S., Dalypov, P.J., 2020. Evaluation of irrigation quality of groundwater in Wamba Sheet 210, north Central Nigeria. *Journal of Geography, Environment and Earth Science International* 61–73. <https://doi.org/10.9734/jgeesi/2020/v24i230203>.
- Spandana, M.P., Suresh, K.R., Prathima, B., 2013. Developing an irrigation water quality index for Vrshabavathi Command area. Available at: [www.ijert.org](http://www.ijert.org).
- Tong, X., Xie, H., Qiu, Y., Zhang, H., Song, L., Zhang, Y., Zhao, J., 2010. Quantitative monitoring of inland water using remote sensing of the upper reaches of the Huangpu River, China. *Int. J. Rem. Sens.* 31 (9), 2471–2492. <https://doi.org/10.1080/01431160902994440>.
- Usali, N., Ismail, M.H., 2010. Use of remote sensing and GIS in monitoring water quality. *J. Sustain. Dev.* 3 (3) <https://doi.org/10.5539/jsd.v3n3p228>.

Wilcox, L.V., 1955. Classification and Use of Irrigation Waters. U.S. Department of Agriculture, United States.

Yıldız, S., Karakuş, C.B., 2020. Estimation of irrigation water quality index with development of an optimum model: a case study. *Environ. Dev. Sustain.* 22 (5), 4771–4786. <https://doi.org/10.1007/s10668-019-00405-5>.

Zhang, W., et al., 2018. Identifying emerging reservoirs along regulated rivers using multi-source remote sensing observations. *Rem. Sens.* 11 (1), 25. <https://doi.org/10.3390/rs11010025>.